1 **BIG regulates dynamic adjustment of circadian period in *Arabidopsis thaliana***

2

3 **Hearn TJ[1], Marti MC[1], Abdul-Awal SM[1,2], Wimalasekera R[1], Stanton CR[1],**

4 **Haydon MJ[3], Theodoulou FL[4], Hannah MA[5] and Webb AAR[1*]**

5

6 [1] Department of Plant Sciences, University of Cambridge, UK, CB2 3EA

7 [2] Biotechnology and Genetic Engineering Discipline, Khulna University, Khulna-

8 9208, Bangladesh

9 [3] School of BioSciences, The University of Melbourne, Victoria 3010, Australia

10 [4] Plant Sciences Department, Rothamsted Research, Harpenden, UK, AL5 2JQ

11 [5] Bayer CropScience SA-NV, Technologiepark 38, 9052 Gent (Zwijnaarde), Belgium

12

13 **Corresponding Author:**

14 AAR Webb, aarw2@cam.ac.uk, +44 (0)1223 333948

15

16 **Short Title:**

17 *BIG* dynamically adjusts the circadian period

18

19 **One-sentence summary:**

1

20 BIG contributes to the dynamic adjustment of the circadian period to establish the

21 correct phase of daily rhythms in Arabidopsis.

22

23 **Author contributions**

24 TH, MJH, MAH and AW devised the study. TH, AA, CS, RM and MM conducted the

25 experiments. TH, MM, FLT, and AW wrote the manuscript.

29

30 **Abstract**

31 Circadian clocks drive rhythms with a period near 24 hours, but the molecular basis

32 of the circadian period's regulation is poorly understood. We previously

33 demonstrated that metabolites affect the free-running period of the circadian

34 oscillator of *Arabidopsis thaliana*, with endogenous sugars acting as an accelerator

35 and exogenous nicotinamide acting as a brake. Changes in circadian oscillator

36 period are thought to adjust the timing of biological activities through the process of

37 entrainment, in which the circadian oscillator becomes synchronised to rhythmic

38 signals such as light and dark cycles, as well as changes in internal metabolism. To

39 identify molecular components associated with the dynamic adjustment of circadian

40 period, we performed a forward genetic screen. We identified Arabidopsis mutants

41 that were either period insensitive to nicotinamide (*sin*) or period oversensitive to

42 nicotinamide (*son*). We mapped *son1* to *BIG,* a gene of unknown molecular function

2

43 that was previously shown to play a role in light signalling. We found that *son1* has

44 an early entrained phase, suggesting that the dynamic alteration of circadian period

45 contributes to the correct timing of biological events. Our data provide insight into

46 how dynamic period adjustment of circadian oscillators contributes to establishing a

47 correct phase relationship with the environment, and they show that BIG is involved

48 in this process.

49

50 **Introduction**

51 The circadian clock is an endogenous oscillator that in *Arabidopsis thaliana* consists

52 of nuclear and cytosolic feedback loops. It is often considered that the circadian

53 oscillator runs with a period of 24-hour but the circadian period is plastic, depending

54 on environmental conditions. For example, in diurnal organisms such as Arabidopsis

55 (*Arabidopsis thaliana*), the circadian clock has a reduced period with increased light

56 intensity (Aschoff 1960). This is commonly referred to as Aschoff's rule and was the

57 foundation for the model of parametric entrainment that describes how the circadian

58 oscillator synchronises with environmental cycles (Aschoff 1960). We have

59 discovered that exogenous application of two common metabolites also regulates

60 circadian period in Arabidopsis. Sucrose reduces circadian period under dim light

61 conditions (Haydon et al., 2013), whereas nicotinamide makes the circadian clock

62 run more slowly, with a period near 27 h (Dodd et al., 2007).

63

64 The way in which circadian clocks regulate and adjust circadian period is unknown.

65 We refer to this ability of the circadian clock to adapt to the environmental conditions

66 as dynamic adjustment of circadian period. To investigate this dynamic adjustment,

3

67 we have used nicotinamide as a tool that increases circadian period. Previously, we

68 have proposed that nicotinamide affects circadian period through its action as an

69 antagonist of Ca^{2+} signalling (Dodd et al., 2007). There is circadian regulation of

70 cytosolic free calcium ($[Ca^{2+}]_{cyt}$) in mesophyll cells (Marti et al., 2013), and this

71 encodes information about light intensity and quality (Xu et al., 2007; Love et al.,

72 2004). In Arabidopsis, circadian regulation of $[Ca^{2+}]_{cyt}$ is driven by the second

73 messenger cyclic adenosine diphosphate ribose (cADPR) under the control of the

74 morning oscillator gene *CIRCADIAN CLOCK ASSOCIATED 1 (CCA1)* (Xu et al.,

75 2007; Dodd et al., 2007). Nicotinamide, the by-product of cADPR synthesis, inhibits

76 both cADPR accumulation (Dodd et al., 2007) and ADPR cyclase activity (Abdul-

77 Awal et al., 2016). There is no gene in Arabidopsis with homology to any of the

78 known ADPR cyclases (Hunt et al., 2007). However, the existence of a completely

79 novel ADPR cyclase in the green lineage cannot be ruled out, as many cyclases are

80 yet to be characterised at the genetic level in mammals (Masuda et al., 1997).

81

82 Nicotinamide increases circadian period in all organisms tested, including

83 Arabidopsis (Dodd et al., 2007), mouse (Asher et al., 2008) and Ostreococcus

84 (O'Neill et al., 2011). In animals, nicotinamide has been hypothesised to affect both

85 circadian period and amplitude through inhibition of poly-ADP-ribose polymerase

86 (PARPs; Ramsey et al., 2008) or SIRTUINs (Asher et al., 2008). Similar to ADPR

87 cyclase, SIRTUINS are enzymes belonging to the NADase superfamily, that release

88 nicotinamide as a by-product with ADPR production. However, consistent with the

89 effect of nicotinamide on circadian period being due to inhibition of ADPR cyclase, a

90 knock out mutation of *CD38*, the main mammalian ADPR cyclase, causes a long

91 circadian period in mice (Sahar et al., 2011).

4

92

We have used nicotinamide as a tool to understand the potential mechanisms that regulate the dynamic adjustment of circadian period and to determine how nicotinamide regulates the circadian clock. We have performed a forward genetic screen to identify loci that affect the sensitivity of the circadian oscillator to nicotinamide. Previous genetic analysis of the circadian system has focused on identification of components of the circadian oscillator through screens for a short or long circadian period in constant light (Millar et al., 1995; Panda et al., 2002; Somers et al., 2000; Hazen et al., 2005) or constant darkness (Kevei et al., 2007; Hong et al., 2010; Martin-Tryon et al., 2007; Ashelford et al., 2011). We have taken a different approach by screening for mutations that are affected in their ability to change circadian period in response to altered conditions. We predicted that such a screen might identify genes involved in the response to nicotinamide and, more importantly, genes that participate in the dynamic adjustment of circadian period. We report the mapping-by-sequencing of an Arabidopsis mutant that is oversensitive to the effect of nicotinamide on circadian period, and identification of the causal mutation in the gene *BIG*. Phenotypic and genotypic analysis of the mutant indicate a wider role for *BIG* in the dynamic adjustment of circadian period. We tested the hypothesis that mutations in this gene that affect dynamic adjustment of free-running period also affect the entrained phase. We find that this dynamic adjustment of circadian period is associated with establishing the correct phase relationship with the environment. Our data therefore identify a genetic component required for the correct regulation of circadian period and suggest that circadian period is not fixed at 24 hours, thus permitting entrainment to different photoperiods. Our screen has provided important

5

116   insight into how circadian clocks entrain to environmental cycles and therefore how

117   plants tell the time.

118

119

6

Results

Forward genetic screen identifies mutants that are compromised in their ability to adjust circadian period in response to nicotinamide

To identify mutants with an altered response of circadian period to nicotinamide, we mutated a Ws-2 dual reporter line with ethyl methanesulphonate (EMS), which generates A-G and C-T transitions in base sequence. This line carries both the *CHLOROPHYLL A/B BINDING PROTEIN2 promoter:LUCIFERASE*[+] (*CAB2:LUC*[+]; Hall et al., 2003) and CaMV 35S promoter*:APOAEQUORIN* (*35S:AEQ*; Xu et al., 2007) reporters. The EMS population was initially screened in the M2 generation for period and amplitude of *CAB2:LUC*[+] in the presence of 10 mM nicotinamide. We used the *CAB2:LUC*[+] reporter because this had previously been used to study the effect of nicotinamide on the Arabidopsis circadian clock (Dodd et al., 2007). By measuring the behaviour of circadian clock output in *CAB2* we could examine the consequence of the entire oscillator dynamics, which is not possible when measuring the behaviour of a single oscillator component. This screen of 16,000 M2 plants identified 372 putative mutants. These mutants were categorized as: i<u>S</u> period <u>I</u>nsensitive to <u>N</u>icotinamide *(sin)*, i<u>S</u> period <u>O</u>versensitive to <u>N</u>icotinamide (*son*)*,* or *i<u>S</u>* <u>A</u>mplitude insensitive to <u>N</u>icotinamide (*san*)*,* based upon a circadian period that was outside of 2 standard deviations of Ws-2 circadian period (*sin* <24.0 h, *son* >26.1 h) or amplitude (*san* >0.40 or <0.18) of *CAB2:LUC*[+] in the presence of 10 mM nicotinamide*.* The nature of the M2 screen meant that in addition to nicotinamide response mutants, it was possible that mutations affecting free-running period could have also been selected.

7

143 We performed a rescreen of the M3 to confirm initial mutants and exclude those that

144 were just free-running circadian period mutants. In the M3 screen, wild-type Ws-2

145 plants responded to 20 mM nicotinamide with an increase in circadian period of

146 *CAB2:LUC*[+] from 23.9 ± 0.2 h to 26.2 ± 0.3 h and amplitude reduced from 1.1 ± 0.04

147 normalised luminescence counts (n.c.) to 0.6 ± 0.03 n.c. (Figure 1a). Sixty-three

148 mutants were confirmed by the rescreening of the M3 generation which also allowed

149 the exclusion of false positives from the M2 screen (Figure 1b, Supplemental Table

150 S1).

151 Twenty-five mutants were confirmed for the *sin* phenotype with either no significant

152 period increase in the presence of 20 mM nicotinamide, or with a reproducibly

153 smaller increase in period than Ws-2 (Supplemental Table S1). Sixteen mutants

154 were confirmed for the *son* phenotype with significantly greater period in the

155 presence of 20 mM nicotinamide compared to Ws-2 (Supplemental Table S1).

156 Similarly, 25 *san* mutants were confirmed to have either no significant decrease in

157 amplitude in response to nicotinamide, or significantly smaller amplitude than Ws-2

158 (Supplemental Table S1).

8

159 The strongest phenotypes (Figure 1c) were seen in *son1* with a nicotinamide-

160 induced circadian period increase of 6.02 ± 0.75 h (*son1* H_2O: 22.6 ± 0.1 h, 20 mM

161 NAM: 28.6 ± 0.7 h, p<0.01 T=8.05), *sin1* with no period increase (*sin1* H_2O: 25.2 ±

162 0.3 h, 20 mM NAM: 25.0 ± 0.3 h, p=0.19 T=0.92) and *san11* which had a circadian

163 period increase of 1.3 h but with a rising amplitude of *CAB2:LUC*[+] compared to

164 damping amplitude in wild type (*san11* H_2O: 1.08 ± 0.03 n.c., 20 mM NAM: 1.05 ±

165 0.0 n.c., T=0.83 p=0.21). The *san* lines all had very low amplitude compared to Ws-2

9
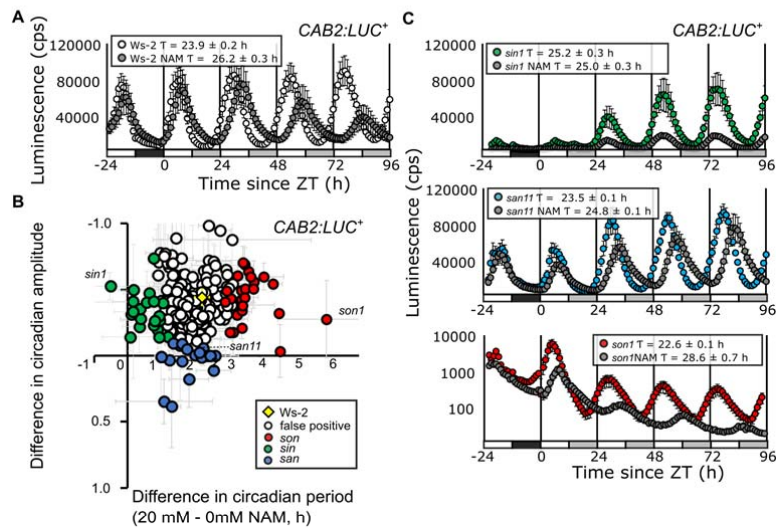
Figure 1

Figure 1. A forward genetic screen separates period and amplitude effects of nicotinamide. (A) *CAB2:LUC⁺* rhythms in wild-type Ws-2 in the presence or absence of 20 mM nicotinamide (NAM) in one entraining 12:12 light dark cycle (Black and white bars) and four days in constant light (white and grey bars). Mean FFT-NLLS period estimates are shown ± SEM (n = 8). **(B)** Free-running circadian period and amplitude difference of M3 plants in a forward genetic screen for the effect of 20 mM nicotinamide on circadian oscillations of *CAB2:LUC⁺*. Period insensitive mutants (*sin*) are indicated in green, period oversensitive mutants (*son*) in red and amplitude sensitive mutants (*san*) in blue. Plants with no detectable nicotinamide-response phenotype in the screen of the M3 population are shown in white, and mean wild-type Ws-2 ± SEM from all experiments (n = 64) is shown overlaid in yellow. Data are pooled from eight separate experiments. (C) *CAB2:LUC⁺* rhythms in *sin1*, *son1* and *san11* mutants (labelled in **B**) in the presence or absence of 20 mM nicotinamide in one entraining 12:12 light dark cycle and four days in 70 μmol m⁻² s⁻¹ constant light (n = 8). Data is representative of two independent experiments in the M3 generation.

166   in the absence of nicotinamide, making the phenotypes difficult to measure robustly

167   and map in segregating populations. Therefore, our laboratory has focussed our

168   attention on the *sin* and *son* period mutant classes.

169   Dose response curves demonstrated that *son1* was hypersensitive to nicotinamide,

170   with significant increases in circadian period with addition of 1 mM nicotinamide

171   (Supplemental Figure S1a; ANOVA: F=6.87 df=15 p=0.02), whilst Ws-2 circadian

172   period of *CAB2:LUC⁺* did not vary significantly until addition of 10 mM nicotinamide

10

173   (ANOVA: F=7.85 df=19 p<0.01). *sin1* was hyposensitive to nicotinamide, as there

174   was no variation in circadian period of *CAB2:LUC⁺* between 0.1 mM and 20 mM

175   nicotinamide (Supplemental Figure S1b; ANOVA: F=2.15 df=18 p=0.11). The

176   mutants were backcrossed twice to the parental Ws-2 line carrying *35S:AEQ* and

177   *CAB2:LUC⁺* for mapping. Here we describe our findings of *son1,* the first mutant that

178   we have mapped from the population, which has the strongest phenotype of all those

179   identified.

180

181   **son1 maps to a mutation in a splice acceptor in BIG**

182   We mapped the causal mutation for *son1* using a mapping population of 25 BC_1F_2

183   plants clearly displaying the mutant phenotype and sequenced pooled DNA to 50-

184   fold coverage. SHOREmap analysis (Schneeberger et al., 2009) using a sliding

185   window of allele frequency identified a region on the long arm of chromosome 3

186   where no recombination had occurred (Figure 2a). Underlying this region was a 750

187   kb interval containing eight SNPs, with three mutations at positions 433767, 474568

188   and 697938 predicted to cause functional changes to gene products (Figure 2b). We

189   confirmed the existence of these SNPs using dCAPs analysis and Sanger

190   sequencing, and fine-mapped the mutation by analysing the segregation pattern in

191   the BC_2F_3 using the M3 screening conditions (Supplemental Figure S2, Figure 2c).

192   When the segregation pattern of the SNPs was compared with the segregation of the

193   *son1* phenotype, the SNP on chromosome 3 at position 433767 was the only SNP

194   that segregated with the *son1* phenotype in the BC_2F_3 (Figure 2c; Supplemental

195   Figure S2, e-f). The wild-type and heterozygous 3:433767 populations were not

196   distinct from one another, with wild type period difference (plus and minus

11

Figure 2

Chr	Position	Ref	Mut	Genomic location	Gene	Type	Ref	Mut
3	114199	C	T	intergenic				
3	187512	C	T	intergenic				
3	433767	C	T	splice_site_change	AT3G02260			
3	451993	C	T	intergenic				
3	474568	C	T	CDS	AT3G02330	Nonsyn	M	I
3	590817	C	T	intronic/noncoding	AT3G02740			
3	871489	C	T	intronic/noncoding	AT3G03610			
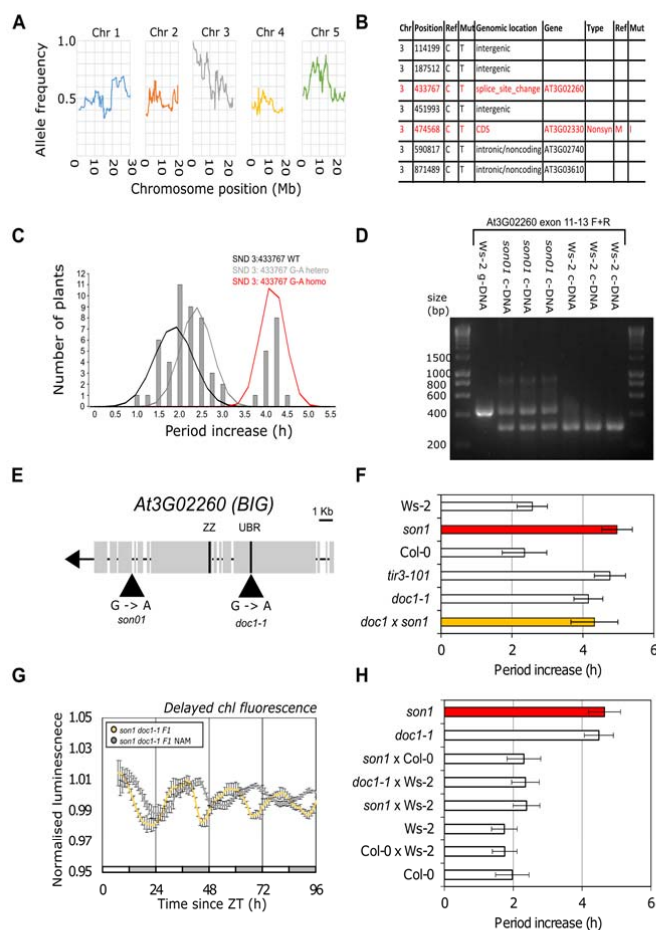
Figure 2. A causal mutation in BIG underlies *son1*

(A) SHOREmap backcross mapping by sequencing analysis of *son1* generated from 25-fold coverage Illumina sequence data obtained from 25 BC_1F_2 individual plants with the son1 phenotype. Individual chromosomes are shown separately with allele frequency sliding window generated with a moving average of 50 Kb. A region with allele frequency of one is found on the long arm of chromosome 3. **(B)** SNPs found on Chromosome 3 in son1 with allele frequency of 1.0. Mutations highlighted in red are predicted to cause a functional change in gene product. **(C)** BC_2F_3 segregation of *son1* phenotype with mutation at 3:433767. Period difference in the presence of 20 mM nicotinamide was calculated by FFT-NLLS and plotted rounded to nearest 0.2 h. Each line consisted of 8 biological replicates, 45 lines were genotyped and phenotyped. Mean and SD for each 3:433767 G-A genotypic sub-population (Wt, heterozygous, and homozygous) were used to plot normal distributions overlaid onto period histogram. **(D)** RT-PCR of *BIG* exons 11 – 12 showing the effect of *son1* on BIG transcript isoforms. Lane 1 has Ws-2 genomic DNA product of predicted size 458bp. Lane 2-4 have *son1* c-DNA products of 314and 458 bp. Lane 5-7 have Ws-2 c-DNA product of 316bp. 1 Kb Ladder annotated with fragment sizes is shown. Independently isolated BC_2F_3 pedigrees were used. **(E)** Gene structure of *At3G02260* (*BIG*), the potential UBR (CRD1) and ZZ zinc finger domains and positions of *son1* and *doc1-1* mutations are labelled. **(F)** Circadian period difference between the presence and absence of 20 mM nicotinamide for delayed chlorophyll fluorescence rhythms in Ws-2, *son1*, Col-0, *doc1-1* and *son1 doc1-1* F1. Period estimates calculated using FFT-NLLS analysis (n = 10). Data are representative of two independent experiments. **(G)** Delayed chlorophyll fluorescence rhythm for *son1* x *doc1-1* F1 in the presence or absence of 20 mM nicotinamide (NAM) across four days in constant light. White and grey bars show subjective day and night. Mean ± SEM shown for n = 10. Data are representative of two independent crosses. **(H)** Circadian period difference between the presence and absence of 20 mM nicotinamide for delayed chlorophyll fluorescence rhythms in of Col-0, Ws-2, Col-0 x Ws-2 F1, *son1*, *doc1*, *son1* x ws-2 F1 and *doc1* x Ws-2 F1. Period estimates calculated using FFT-NLLS analysis (n = 10).

197   nicotinamide) of 1.9 ± 0.5 and heterozygous period difference of 2.5 ± 0.4 h

12

198   compared to the homozygous 3:433767 period difference of 4.3 ± 0.3 h.

199   This SNP resulted in a G-A transition causing a mutation in the 3' splice acceptor site

200   of exon 12 of *At3G02260* (Figure 2d). *At3G02260* encodes BIG, a callosin-like

201   protein of 5098 amino acids and unknown molecular function (Gil et al., 2001). The

202   M3 line carrying *son1* is slightly short period (Figure 1). This short period phenotype

203   in the M3 generation was reproducible but not significant (period diff = 0.53, p>0.05,

204   Supplemental Figure S3). However, the short period phenotype was not present in

205   the M4 generation, or in the BC_1F_3 (Supplemental Figure S3) or BC_2F_3

206   (Supplemental Figure S2), indicating that the phenotype was not linked to the *son1*

207   phenotype after backcrossing to Ws-2 and that the *son1* mutation does not cause a

208   classical circadian period phenotype

209

210   To test the effect of the 3:433767 mutation on transcript splicing in the *son1* mutant,

211   PCR products were amplified from cDNA using primers spanning exon 11 - 12 of

212   *BIG* in three independent BC_2F_3 pedigrees. In addition to the 316 bp product

213   amplified from wild-type cDNA (Figure 2d, lane 6-8), an additional product was

214   amplified from *son1* mutants (Figure 2d, lane 3-5) that was of equivalent size to the

215   458 bp PCR product amplified from wild-type genomic DNA (Figure 2d lane 2),

216   indicating that it represented an unspliced transcript. Sequencing of both *At3G02260*

217   splice variants in *son1* demonstrated that there was a G-A transition corresponding

218   to 3:433737 in both products (Supplemental Figure S4). The smaller fragment was 2

219   bp smaller than the Ws-2 product, with a second AG immediately downstream of the

220   first being used as a splice acceptor instead, whilst the larger 458 bp product

221   contained the full sequence of intron 11 - 12 suggesting it is retained in *son1*, due to

13

222 inefficient splicing. Thus, the G-A 3:433767 causes both the production of an

223 unspliced transcript, and the use of a cryptic splice site in *son1,* both of which result

224 in frameshifts and are predicted to cause premature stop codons.

225

226 To confirm that the *son1* phenotype was due to the G to A transition in *BIG*, we

227 assessed the response to nicotinamide in mutants in *BIG* identified from previous

228 mutant screens, *dark over-expresser of cab1-1* (*doc1-1)* (Li et al., 1994) and *auxin*

229 *transport inhibitor response 3* (*tir3-101)* (Ruegger et al., 1997), using delayed

230 chlorophyll fluorescence (Gould et al., 2009). *doc1-1* has an increase in

231 photosynthesis-related gene expression, including *CAB* genes, in etiolated seedlings

232 in the dark (Li et al., 1994; Gil et al., 2001) caused by a G-A transition resulting in a

233 Cys to Thr amino acid substitution in the first cysteine rich domain (CRD-1, also

234 known as a UBR box). *tir3*-101 is reported to have impaired polar auxin transport

235 giving rise to a dwarf phenotype (Ruegger et al., 1997; Prusinkiewicz et al., 2009).

236 Both *doc1-1* and *tir3-101* were oversensitive to nicotinamide compared to their

237 respective wild types (Figure 2f, Supplemental Figure S5; Col-0: 2.9 ± 0.5 h, *doc1-1*:

238 4.5 ± 0.4 h, *tir3-101* 4.4 ± 0.9 h). The increased response of circadian period in the

239 three different *son1*, *doc1-1* and *tir3-101* alleles of *BIG* suggested that the mutations

240 in *BIG* are causal for the nicotinamide oversensitive phenotype, and none have a

241 circadian period phenotype in constant high light.

242 As confirmation, we tested whether *son1* is allelic to *doc1-1.* The *doc1-1 son1* F1

243 plants had significantly greater period increase in the presence of nicotinamide (4.3 ±

244 0.7 h) than either Ws-2 (1.7 ± 1.2 h, T=2.22, df=19, p<0.05) or Col-0 (2.4 ± 0.6 h,

245 T=2.16, df=19, p<0.05), and were not statistically different to either *doc1-1* (4.2 ± 0.4

14

246   h; T=0.22, df=19, p=0.42) or *son1* (4.9 ± 0.4 h, T=0.81, df=19, p=0.21) in the

247   presence of 20 mM nicotinamide (Figure 2f - g). To control for ecotype or dominance

248   effects we analysed delayed fluorescence in the presence and absence of

249   nicotinamide for F1 of crosses between *son1* and Ws-2, *son1* and Col-0 and *doc1*

250   and Ws-2 (Figure 2h, Supplemental Figure S6). These crosses all behaved as wild-

251   type, and had circadian period increases that corresponded to the heterozygous

252   BC_2F_3 on the segregation analysis (Figure 2c). This demonstrates that *doc1-1* is

253   allelic to *son1* and that *BIG* regulates sensitivity of the circadian oscillator to

254   nicotinamide.

255   Having established that *son1* and *doc1-1* are both nicotinamide-oversensitive for

256   circadian period, we tested whether *son1* plants exhibit the *doc1* phenotype of

257   increased photosynthesis related gene expression in etiolated seedlings in the dark

258   (Li et al., 1994; Gil et al., 2001). *CAB2:LUC*[+] expression was higher in etiolated

259   seedlings of *son1* than wild type in constant dark (DD) (Supplemental Figure S7 a-c),

260   indicating that *son1* also had a dark-over expresser of *CAB* phenotype consistent

261   with allelism to *doc1-1.* Similar to *doc1-1,* higher *CAB2* expression in constant dark

262   was not associated with premature de-etiolation (Supplemental Figure S7 d-e).

263   To test if BIG could be part of the transcriptional feedback loops of the oscillator we

264   looked at the transcript profile for *BIG* in the publicly available diurnal transcriptomic

265   datasets under long and short days (Supplemental Figure S8). *BIG* does not oscillate

266   in either long or short photoperiods in two separate 48 h microarray experiments

267   (Endo et al., 2014; Mockler et al., 2007). The abundance of *BIG* transcript also does

268   not appear to be regulated by the circadian oscillator, with no detectable oscillations

269   using JTK cycle (p>0.05) in a circadian transcriptome taken over 48 hours in

270   constant conditions (Dalchau et al., 2010). The lack of circadian or diel changes in

15

271   *BIG* transcript abundance suggests BIG is not part of transcriptional feedback loops

272   in the circadian oscillator.

273   *son1* affects circadian $[Ca^{2+}]_{cyt}$ signalling

274   In addition to increasing circadian period, nicotinamide abolishes circadian regulation

275   of $[Ca^{2+}]_{cyt}$, potentially through inhibition of the ADPR cyclase activity that generates

276   the Ca^{2+} agonist cADPR (Dodd et al.*, 2007; Abdul-Awal et al.*, 2016). We

277   investigated the effect of *son1* on Ca^{2+} signalling using the 35S:AEQ reporter. In Ws-

278   2 there was sinusoidal circadian regulation of $[Ca^{2+}]_{cyt}$ which had an estimated period

279   of 24.2 ± 0.9 h and RAE of 0.3 ± 0.0 (Figure 3a). *son1* affected the circadian

280   regulation of $[Ca^{2+}]_{cyt,}$ leading to a non-sinusoidal oscillation with an increasing basal

281   level and dampening over time. This resulted in fast Fourier transform-non-linear

282   least squares (FFT-NLLS) analysis estimating the rhythm as only weakly rhythmic

283   with an RAE of 0.5 ± 0.1 (period = 23.1 ± 0.2 h; Figure 3a). Both *son1* and Ws-2

284   circadian $[Ca^{2+}]_{cyt}$ signals were inhibited by 20 mM nicotinamide (Figure 3b; Ws-2:

285   RAE = 0.7 ± 0.1; *son1:* 0.7 ± 0.1).

286   Because we have proposed previously that circadian regulation of $[Ca^{2+}]_{cyt}$ arises

287   from cADPR-mediated Ca^{2+} release, we measured the activity of ADPR cyclase in

288   wild type and mutant. *son1* had significantly higher ADPR cyclase activity compared

289   to Ws-2, (p=0.01) in the middle of the photoperiod representing peak $[Ca^{2+}]_{cyt}$ (Figure

290   3c). $[Ca^{2+}]_{cyt}$ was also elevated at the same time point in *son1* compared to Ws-2

291   (Figure 3d; p<0.05). This effect was more pronounced after 72 h in constant light,

292   where the LL 35S:AEQ data had previously indicated there to be a much higher

293   basal level of $[Ca^{2+}]_{cyt}$ (p<0.05). $[Ca^{2+}]_{cyt}$ at both time points was reduced by

294   incubation with 20 mM nicotinamide (Figure 3d). Thus, although nicotinamide

16
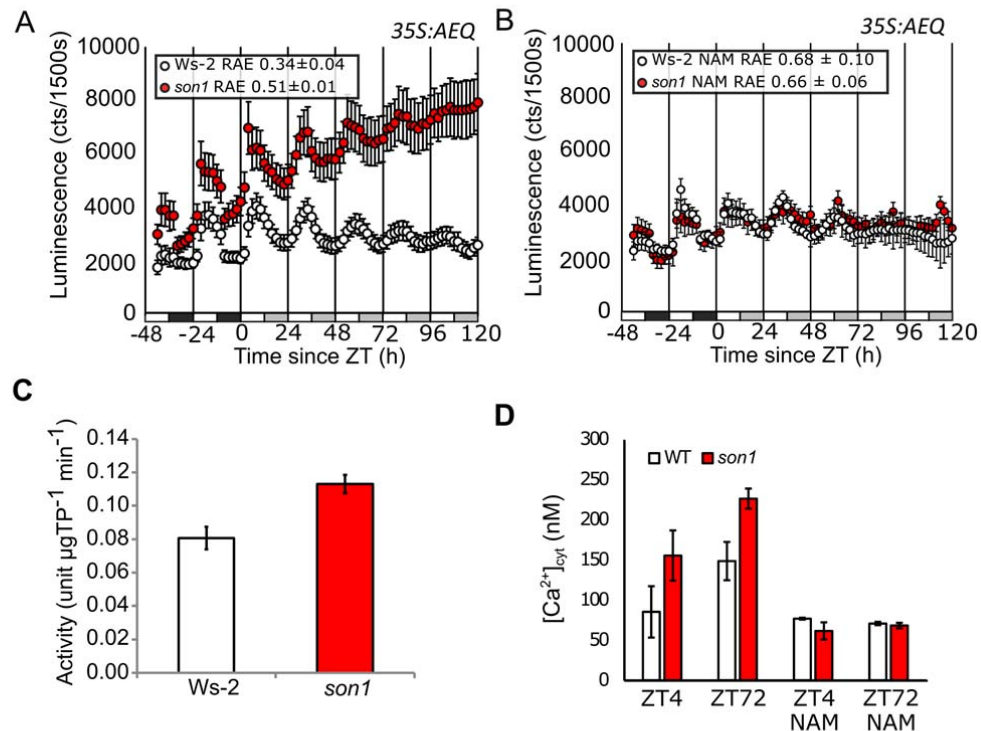
Figure 3

Figure 3. *son1* affects circadian [Ca²⁺]꜀ᵧₜ signals

Bioluminescence (photon counts/1500 seconds) from *son1* and Ws-2 expressing *35S:AEQUORIN* across two light dark cycles and five days in constant 70 μmol m⁻² s⁻¹ white light grown on 20 mM mannitol **(A)** or 20 mM nicotinamide **(B)**. Mean ± SEM, n = 8. Data are representative of three independent experiments in the BC₂F₃ generation. **(C)** ADPR cyclase activity measured using NGD assay at ZT4 in 70 μmol m⁻² s⁻¹ white light from 3-4 week old Ws-2 (white) and *son1* (red) seedlings, mean of 3 biological replicates shown with SEM. **(D)** [Ca²⁺]꜀ᵧₜ measured at ZT 4 and ZT72 in constant 70 μmol m⁻² s⁻¹ white light from 11 and 14 day old Ws-2 (white) and *son1* (red) seedlings respectively , n=12 . Data are representative of three independent experiments in the BC₂F₃ generation.

295   reduced $[Ca^{2+}]_{cyt}$ to similar concentrations in wild-type and *son1*, the change in

296   $[Ca^{2+}]_{cyt}$ in *son1* was greater as untreated plants have higher $[Ca^{2+}]_{cyt}$, indicating that

297   the $[Ca^{2+}]_{cyt}$ increase in *son1* might be ADPR cyclase-dependent.

298

299   ***son1* affects circadian oscillator gene expression**

17

300 Circadian clocks evolved to provide competitive advantage in light and dark cycles

301 and therefore, to investigate the role of *BIG* in the daily timing of Arabidopsis we

302 examined the effect of *son1* on oscillator gene transcript abundance in light and dark

303 cycles and in constant light. As our phenotype was based on the *CAB2* gene, we

304 measured abundance of *CCA1*, a main circadian regulator of *CAB2*, and also the

305 direct regulators of *CCA1* – *TOC1*, *PRR7* and *CHE*. *son1* affected circadian

306 oscillator transcript levels in light dark cycles. The expression of *CCA1* immediately

307 before dawn was higher in *son1* compared to Ws-2 (Figure 4a; p<0.01) which

308 corresponded to a reduction in *TOC1* expression immediately before dusk (Figure

309 4a; p=0.01) and with a significant reduction in *CHE* expression at both dawn and

310 dusk in *son1* (Figure 4a; p<0.01). We also measured the expression of *CCA1*,

311 *TOC1*, *CHE* and *PRR7* in constant light across a 48 h time course in *son1* and Ws-2

312 in the presence and absence of 20 mM nicotinamide and estimated circadian period

313 using JTK-cycle (Hughes et al., 2010). We performed this to confirm the *son1*

314 phenotype at the level of gene expression and identify if there were any changes in

315 gene expression between mutant and wild-type in the absence of nicotinamide

316 (Figure 4b). In Ws-2, nicotinamide treatment significantly reduced the peak

317 expression of all the genes in the first cycle (p<0.05). Nicotinamide also significantly

318 reduced peak *CCA1* and *PRR7* transcript levels in *son1,* however there was no

319 significant change in *TOC1* and *CHE* at any time point. In *son1*, *CCA1* and *PRR7*

320 rhythms had an increased circadian period in the presence of nicotinamide

321 compared to Ws-2, with period of 28 h in *son1* (p<0.001) but 24 h in wild-type

322 (p<0.001). *CHE* was not rhythmic with JTK-cycle in either Ws-2 (p=1) or *son1*

323 (p=0.08)*. TOC1* was rhythmic with JTK-cycle in Ws-2 with period of 24 h (p<0.05)

324 but not rhythmic in *son1* (p=0.16). Thus, the *son1* phenotype can be seen in rhythms

18
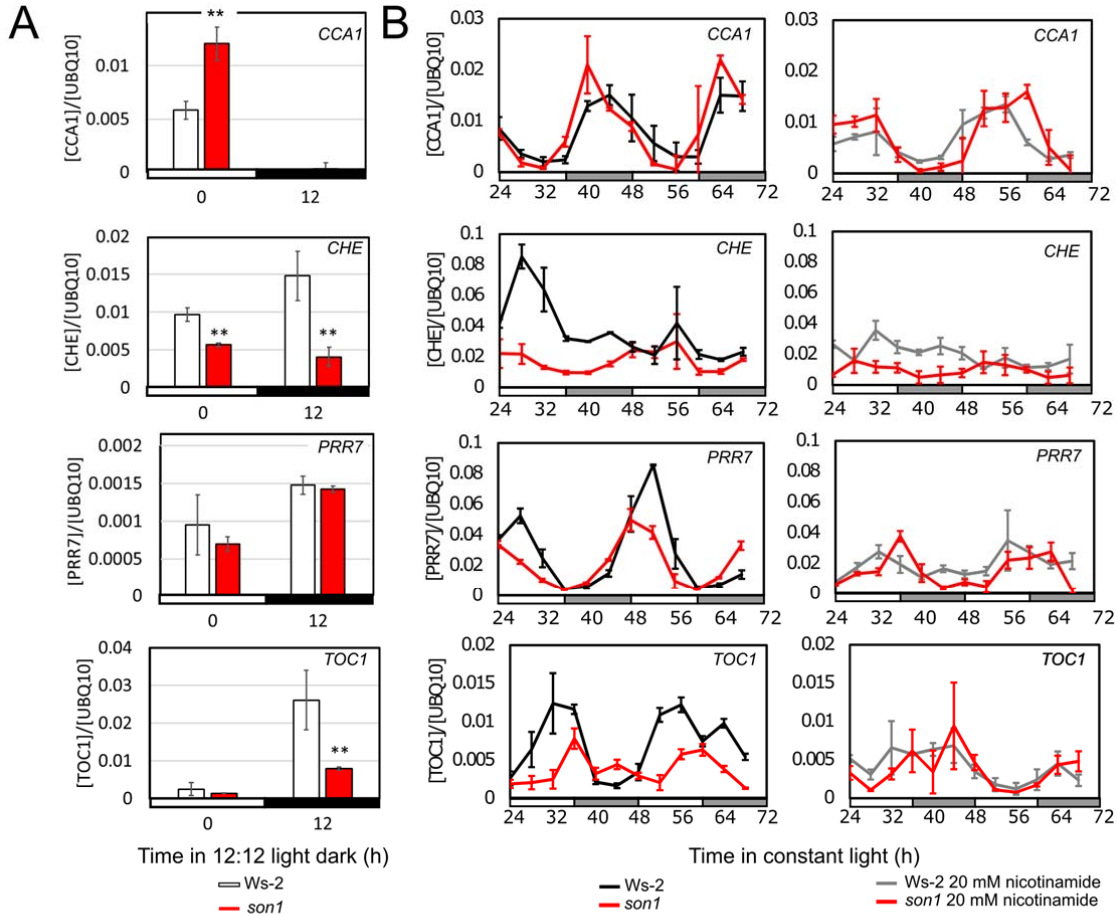
Figure 4

Figure 4. *son1* affects circadian clock gene expression in LD and constant light

(A) *CCA1*, *PRR7*, *TOC1* and *CHE* expression from *son1* (red) and Ws-2 (white) samples harvested immediately preceding dawn (ZT0) and dusk (ZT12).

(B) *CCA1*, *PRR7*, *TOC1* and *CHE* expression from Ws-2 and *son1* in the absence (left) and in the presence of 20 mM nicotinamide (right) across 48 hours in constant 70 μmol m^{-2} s^{-1} light from ZT24 – ZT72. Relative expression of genes normalised to UBQ10f expression is given ± standard deviation [n=3]. Plants were grown as clusters of 5 plants for 11 days in light dark cycles prior to experiment.

325   of *CCA1* and *PRR7,* but in the presence of nicotinamide rhythms of *CHE* and *TOC1*

326   were suppressed with *TOC1* also being suppressed in *son1* in the absence of

327   nicotinamide.

19

328 ***son1* affects dynamic period adjustment of the circadian oscillator to regulate**

329 **the entrained phase**

330 As *son1* is compromised in the ability to regulate changes in circadian period in

331 response to nicotinamide, we tested whether it was also affected in its ability to

332 adjust period correctly to other stimuli. Response to light is the most well

333 characterised dynamic adjustment of the circadian period and is described by

334 Aschoff's rule (Aschoff 1960). We tested the hypothesis that *son1* might be

335 compromised in the ability to regulate circadian period at different light intensities by

336 performing a fluence response curve (Figure 5a).

337 There was no difference between the period length of *CAB2:LUC*$^+$ rhythms in Ws-2

338 and *son1* at 100 µmol m^{-2} s^{-1} light (Ws-2: 23.2 ± 0.1 h, *son1*: 23.0 ± 0.1 h,) which

339 was the intensity of light used for entrainment, indicating again that *son1* is not a

340 circadian period mutant. However, *son1* had a significantly shorter circadian period

341 compared to wild type under low fluence rates (Figure 5a, Supplemental Figure S9):

342 under 5 µmol m^{-2} s^{-1} light *son1* had a period of 26.6 ± 0.8 h and Ws-2 had a period of

343 29.0 ± 0.3 h (p<0.01, Figure 5b). This indicates that *son1* cannot properly regulate

344 circadian period in response to changes in light intensity. A similar phenotype was

345 detected in *doc1-1*. Under 5 µmol m^{-2} s^{-1} light *doc1-1* had a circadian period of

346 *CAB2:LUC*$^+$ of 25.7 ± 0.1 h and Col-0 had a period of 29.2 ± 0.2 h (p<0.01,

347 Supplemental Figure S9).

348 Having previously established that *son1* affects the expression of circadian clock

349 genes in a light and dark cycle, we next investigated the effect of *son1* on the

350 entrained phase to investigate the potential roles of *BIG* in the daily timing of

351 Arabidopsis. Wild-type Ws-2 had a typical phase shift of later phase with increasing
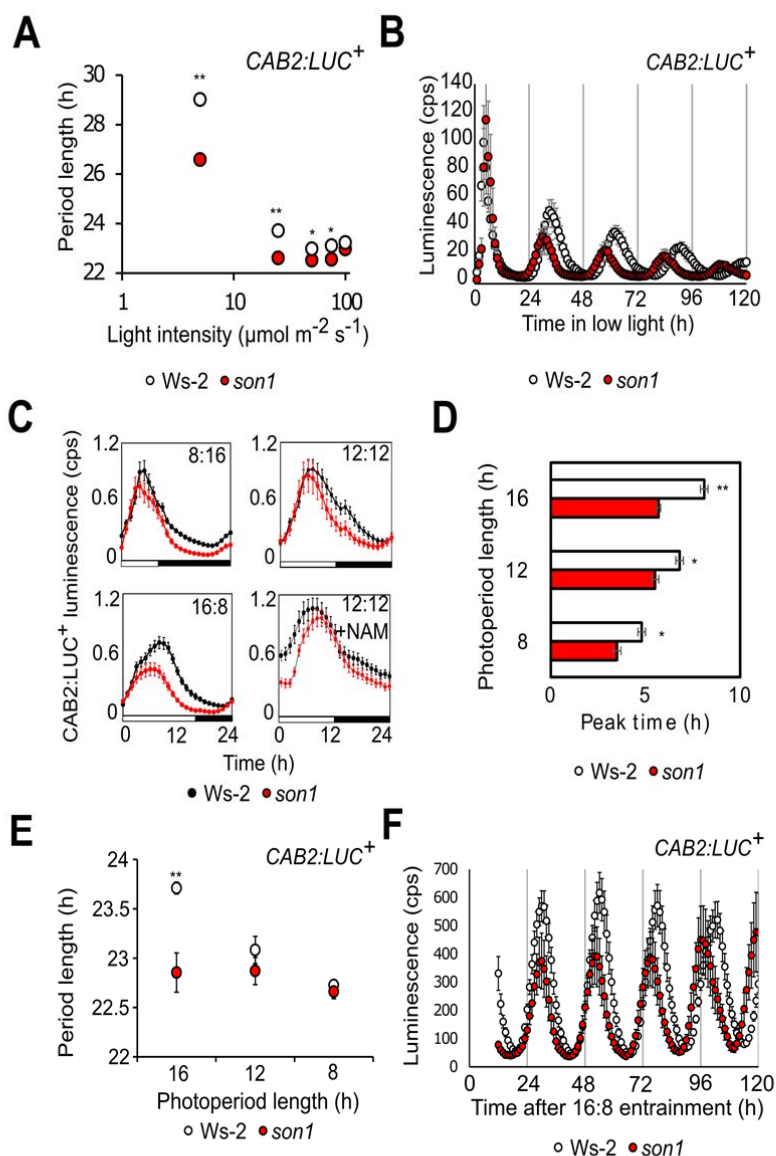
20

Figure 5

Figure 5. *son1* affects dynamic circadian period adjustment by light and photoperiod
(A) Fluence response curve for circadian period of *CAB2:LUC*$^+$ in Ws-2 and *son1* estimated in equal mix red and blue light (Mean ± SEM, n = 8-12). Data are pooled from three independent experiments. **(B)** *CAB2:LUC*$^+$ rhythm of *son1* and Ws-2 assayed over five days in constant 5 μmol m^{-2} s^{-1} equal mix red and blue light (Mean ± SEM, n = 8). Data are representative of two independent experiments in the BC$_2$F$_3$ generation. In Figure 4a the small error bars are obscured by symbols. **(C)** *CAB2:LUC*$^+$ luminescence (counts s-1) from *son1* (red) and Ws-2 (black) seedlings grown in 8:16, 12:12 and16:8 photoperiods. Plants grown in 12:12 were treated with media supplemented with or without 20 mM nicotinamide (NAM) 2 days prior to entrainment in camera chamber (Mean ± SEM, n=8). Plants were grown in entrainment conditions since germination, and transferred to camera chamber one day before imaging, maintaining the same entrainment regime. Data are representative of three independent experiments. **(D)** Peak time of *CAB2:LUC*$^+$ from LD cycles in **(C)**.
(E) Photoperiod response curve for circadian period of *CAB2:LUC*$^+$ in Ws-2 and *son1* estimated in equal mix 80 μmol m^{-2} s^{-1} red and blue light (Mean ± SEM, n = 8). Data are pooled from two independent experiments. Plants were entrained in either photoperiods of either 16, 12 or 8 hours prior to transfer to constant light. **(F)** *CAB2:LUC*$^+$ rhythm of *son1* and Ws-2 entrained in 16:8 LD cycles and released into constant light for five days (Mean ± SEM, n = 8).

352   photoperiod (Figure 5c, peak at 4.8 ± 0.2 h (8:16), peak at 6.8 ± 0.2 h (12:12) peak
21

at 8.1 ± 0.2 h (16:8). By contrast, *son1* was an early phase mutant (Figure 5c-d,

peak at 3.5 ± 0.2 h (8:16), peak at 5.5 ± 0.2 h (12:12) peak at 5.7 ± 0.1 h (16:8).

These data demonstrate that *BIG* is required for correct circadian entrainment.

Lastly, we measured the effect of nicotinamide on entrained phase under 12:12

(Figure 5c), and found that it caused a phase delay of *CAB2:LUC*[+] peak expression

of 1 h in Ws-2 and 3 h in *son1* (Ws-2: ZT 7.8 ± 0.2, *son1*: ZT 8.8 ± 0.2), consistent

with the effect of nicotinamide on free running-period in both backgrounds.

Finally, having identified that BIG regulates dynamic adjustment of circadian period

and that it is required for correct circadian entrainment, we wanted to investigate

whether oscillator period is associated with entrainment and whether the effect of

BIG on phase could be involved in this regulation. To do this, we studied whether

entrainment photoperiod affects free-running period in Ws-2 and *son1* (Figure 5e).

The results showed that there is a relationship between length of entrainment

photoperiod and the length of circadian period in Ws-2 (Figure 5e). However, this

relationship was lost in *son1*, whose circadian period was not affected by the

duration of the photoperiod during entrainment. As a result of this, *son1* did not have

significantly shorter free-running period of *CAB2:LUC*+ compared to Ws-2 when

released from entrainment cycles of 8:16 and 12:12 (*son1*: 22.6 ± 0.07 h (8:16), 22.8

± 0.14 h (12:12); Ws-2: 22.7 ± 0.04 h (8:16), 23.1 ± 0.14 h (12:12). However, when

plants were entrained in 16:8 *son1* had free-running period of 22.7 ± 0.2 h, an hour

shorter than Ws-2 (23.7 ± 0.06 h, p<0.05; Figure 5f). This shows that the

photoperiod-determined entrained phase of the circadian clock affects the free-

running period in constant light, and *son1* does not adjust circadian period correctly

in 16:8. We performed the same series of experiments but with circadian free-run in

22

378   constant darkness, in the presence of sucrose to sustain the oscillation of

379   *CAB2:LUC*[+] (Dalchau et al., 2011). Similar to the result in constant light, we saw that

380   in wild-type plants free-running period length increased with longer entraining

381   photoperiod (Supplemental Figure S10), and for plants entrained in 16:8 *son1* had

382   significantly shorter free-running period than wild-type (Ws-2: 27.0 ± 0.4 h; *son1*:

383   25.7 ± 0.5 h; p<0.05).

384   Thus, *son1* cannot correctly adjust period and has impaired phase in response to

385   photoperiod. Collectively, these data demonstrate that nicotinamide targets a

386   pathway involved in establishing the phase relationship between the circadian

387   oscillator and the external environment and that *BIG* contributes to the correct timing

388   of physiology in light and dark cycles, through regulating the pace of the oscillator.

23

Discussion

Using a forward genetic screen, we found that *BIG* is a regulator of the dynamic

adjustment of circadian period and phase. The period of the circadian oscillator is not

fixed to 24 hours, but instead is a dynamically plastic phenotype and dependent on

environmental conditions. Typically, experimentalists measure circadian period in

constant conditions that allow the circadian oscillator to free run. In these constant

conditions, the period of the Arabidopsis circadian oscillator decreases with

increasing light intensity (Somers et al., 1998a), temperature (Salome et al., 2010)

and sucrose (Haydon et al., 2013) and increases with nicotinamide (Dodd et al.,

2007). We have identified a nicotinamide over-sensitive phenotype resulting from a

mutation in *BIG*. *son1* is allelic to *doc1-1,* a previously characterised mutation in *BIG*

confirming that *BIG* is a regulator of the sensitivity of the circadian oscillator to

nicotinamide.

Whilst NAD is an abundant metabolite, we do not suggest that cellular nicotinamide

derived from NAD breakdown directly regulates the pace of the circadian oscillator

as part of the normal functioning of the plant. Instead, we consider nicotinamide as a

probe that can be used to understand the potential mechanisms by which the

circadian oscillator dynamically adjusts circadian period. Previously, we proposed

that nicotinamide affects circadian period through the inhibition of ADPR cyclase

activity and therefore the production of cADPR, which is a Ca^{2+} agonist (Dodd et al.,

2007; Abdul-Awal et al., 2016). Our demonstration that mutations in *BIG* affecting the

sensitivity of the circadian oscillator to nicotinamide also affect the regulation of

$[Ca^{2+}]_{cyt}$ are supportive of the hypothesis that nicotinamide regulates circadian period

25

414   through a Ca^{2+}-sensitive mechanism. *son1* has higher $[Ca^{2+}]_{cyt}$ and ADPR cyclase

415   activity than wild-type, and that increased $[Ca^{2+}]_{cyt}$ is nicotinamide-sensitive. This

416   might indicate that increased effect of nicotinamide on circadian period is related to

417   the altered $[Ca^{2+}]_{cyt}$ in the mutant. However, we do not exclude the possibility of

418   additional Ca^{2+}-insensitive modes of action of nicotinamide on the circadian system

419   (Malapeira et al., 2012).

420   Animal homologues of BIG, UBR4/p600 in mammals and Calossin/Pushover in

421   Drosophila, are confirmed calmodulin-binding proteins (Xu et al., 1998; Nakatani et

422   al., 2005; Belzil et al., 2013) and have been proposed to act as part of a Ca^{2+}

423   sensing/signalling mechanism. In mammalian neurons, UBR4, calmodulin and

424   calmodulin-dependent protein kinase IIα form a complex upon glutamate-induced

425   Ca^{2+} entry through NMDA receptors or inositol trisphosphate receptor-mediated Ca^{2+}

426   release from the ER (Belzil et al., 2013). Since BIG has a putative calmodulin binding

427   domain (Yap et al., 2000), it is tempting to speculate that this could also play a role in

428   Ca^{2+} signalling, although the interacting molecular players will be different in plants.

429

430   *BIG* was originally identified as a light signalling regulator (Li et al., 1994), and was

431   later shown to also control multiple hormone signalling pathways (Kanyuka et al.,

432   2003), including auxin transport (Guo et al., 2013), and has recently been implicated

433   in CO_2-induced stomatal closure (He et al., 2018). The precise biochemical functions

434   of BIG are unknown but mutations in *Pushover* and knockout or down-regulation of

435   UBR4 also produce pleiotropic phenotypes (Richards et al., 1996; Sekelsky et al.,

436   1999; Yager et al., 2001; Nakatani et al., 2005; Belzil et al., 2014). BIG, UBR4 and

437   Pushover contain a zinc finger-like domain, the UBR box, found in ubiquitin E3

26

438   ligases specific to the N-end rule for targeted protein degradation (Gil et al., 2001;

439   Tasaki et al., 2005; 2009). The N-end rule is a conserved pathway in which proteins

440   are targeted for destruction dependent on their N-terminal residue and has diverse

441   roles in different organisms (Bachmair et al., 1986; Gibbs et al., 2014). Whilst UBR4

442   is required for degradation of model and physiological N-end rule substrates, it

443   contains no HECT or RING domains and hence is considered unlikely to act as an

444   E3 ligase in isolation, rather, it may act as a substrate (N-degron) recognition subunit

445   of a complex (Tasaki et al., 2005; 2009). It is not known whether BIG belongs to an

446   E3 ligase complex or whether it has intrinsic E3 ligase activity. Direct evidence for

447   the ability of the recombinant UBR box of mammalian UBR4 to bind N-degrons is

448   lacking (Tasaki et al., 2009) but previous bioinformatics analysis identified a ZZ

449   domain in BIG (Gil et al., 2001). The ZZ domain is structurally and evolutionarily

450   related to the UBR box (Kaur and Subramanian, 2015) and has recently been shown

451   to bind N-degrons in the autophagic adaptor protein p62 (Cha-Molstad et al., 2017).

452   There is a precedent for regulation of circadian period through control of protein

453   turnover since a double mutant lacking two ubiquitin-specific proteases UBP12 and

454   UBP13 exhibits a short period circadian clock phenotype (Cui et al., 2013). Thus,

455   one potential mode of action of BIG on the circadian oscillator is through a role in

456   protein degradation, but further study will be required to confirm or reject this

457   hypothesis.

458   The effect of the *son1* mutation on levels of $[Ca^{2+}]_{cyt}$ was greater during the night or

459   subjective night than during the day or subjective day. This is indicative of a time-

460   dependent effect of BIG in the circadian system. Similarly, the *doc1-1* allele of *BIG*

461   specifically affects the expression of *CAB* and other photosynthetic genes at night,

462   rather than in the day. These data suggest that *BIG* acts at night in the circadian

27

463   system. Previous studies have demonstrated that *BIG* plays a role in conveying light

464   information, and partially suppresses the phenotype of *phytochromeA* and

465   *phytochromeB* mutations on hypocotyl length (Kanyuka et al., 2003). Thus, *BIG* may

466   be involved in conveying light signalling for circadian entrainment. However, it is

467   likely that *BIG* regulates period or entrainment more widely, due to the effect of *son1*

468   on both nicotinamide period lengthening, and photoperiod regulation of period,

469   indicating that *BIG* has a further role outside of light signalling.

470   Time-dependent effects on the circadian oscillator are also sometimes associated

471   with entrainment, which is the matching of the phase and period of the oscillator with

472   that of the external photoperiod. Synchronisation of the circadian oscillator through

473   entrainment ensures that cellular events occur at the right time of day and ensures

474   that the circadian oscillator can track dawn and dusk as they change through the

475   year. This is essential to co-ordinate whole organism responses as circadian period

476   is different between organs (Takahashi et al., 2015), and is age dependent (Kim et

477   al., 2016). We found that *son1* has an early entrained phase in long day cycles,

478   suggesting an impact on entrainment. The early phase of *son1* and the reduced

479   ability to dynamically alter circadian period to light and nicotinamide might be related

480   through parametric entrainment. The inability of *son1* to adjust period depending on

481   entrainment photoperiod strongly suggests this. A previous study demonstrated that

482   tissue-specific changes in circadian period are accompanied by corresponding

483   changes in entrained phase (Takahashi et al., 2015). The effect of photoperiod on

484   the entrained phase of the oscillator has been widely reported (Yeang 2015, Millar

485   and Kay 1996, and Millar et al., 2015). Importantly, Millar et al., 2015 report that the

486   circadian mutant *cca1 lhy* has the same phase under 8:16, 12:12 and 16:8

487   photoperiods and thus is unable to adjust phase to entrainment photoperiod unlike

28

488   the wild-type which had a 2.6 h difference. This is similar to the result we find here

489   for *son1* which has the same phase under 12:12 and 16:8 photoperiods. Unlike

490   *CCA1,* the transcript of *BIG* does not oscillate either in light dark cycles or in

491   constant light, and shows no modulation by photoperiod. This indicates that *BIG* is

492   not part of the transcription-based oscillator loops.

493   When previously identified Arabidopsis circadian mutants are viewed in the context

494   of phenotypic plasticity to light, they can be assigned to one of four categories

495   (Supplemental Table S2). Mutants can have a constitutive effect on circadian period

496   at all intensities of light and the mutation therefore has no effect on dynamic plasticity

497   of the circadian oscillator. Alternatively, mutants might have no plastic response to

498   light, appearing insensitive with period unchanging at all light intensities. Finally,

499   using the conventions in the literature (Martin-tryon et al 2008) we have defined

500   mutations as hyposensitive, with is a shallow response curve to light, or

501   hypersensitive in which the response curve is steep. Ten mutations do not affect

502   dynamic adjustment to either red or blue light, including four mutations that do not

503   affect the response to both wavelengths: the *toc1*-1 allele (Somers et al., 1998a),

504   *cry2-1* (Somers et al., 1998b), *fio1-1* (Kim et al 2008) and *tej* (Panda et al., 2002).

505   There are eight mutations reported to cause insensitivity to either red or blue light

506   including *prr7-11* to red light (Farre et al., 2005) and *gi-200* (Martin-Tryon et al.,

507   2007) to both red and blue light. Seven mutations cause hypersensitivity to either red

508   or blue light including *toc1-2* (Martin-Tryon and Harmer 2008), *lwd1 lwd2* (Wang et

509   al., 2011), and light signalling mutants *phyA-201* and *cry1-1* (Somers et al., 1998b).

510   The "hypersensitivity" in terms of the effect of light on circadian period for *phyA-201*

511   and *cry1-1* is caused by a very steep fluence response curve due to the inability to

512   sense low light intensities. However, only three reported mutations cause

29

513   hyposensitivity to light. *rve4 rve6 rve8* (Gray et al., 2017) and *phyB-1* (Somers et al.,

514   1998b) confer hyposensitivity to red light, and *prr7-3* to blue light (Farre et al., 2005).

515   The phenotype of *son1* for the white light fluence response curve is also

516   hyposensitive. However, as shown in Supplemental Table S2, *rve4 rve6 rve8* (Gray

517   et al., 2017) and *phyB-1* (Somers et al., 1998b) both have long period phenotypes in

518   addition to hyposensitivity phenotypes whereas *son1* has no period phenotype under

519   the light intensity used for the initial entrainment in 12:12 (Figure 5; Supplemental

520   Figure S3). Thus, the phenotype of *son1* indicates a function in adjusting period to

521   stimuli, rather than being a core oscillator component, as under normal conditions

522   there is no evidence for it being an oscillator component, since period defects are

523   conditional, and the transcript abundance does not oscillate. The short period of

524   *son1* after entrainment only to long days, or through maintenance in constant low

525   light (Figure 5) demonstrates that the effect of *son1* is conditional on environmental

526   input, suggesting that BIG is associated with regulation of plastic period of the

527   oscillator by environmental signals, rather than acting as a core oscillator

528   component. There is variability in the reported phenotypes of *prr7* mutants, with them

529   being described as long period (Farre et al., 2005) or wild type (Nakamichi et al.,

530   2005; Seki et al., 2016). This and the hyposensitivity to light suggest that *prr7*

531   mutants might also have a defect in plasticity similar to *son1* in terms of responses to

532   light. The mechanisms might be different because PRR7 is an oscillator component,

533   whilst there is no evidence for BIG being so.

534   Alterations in circadian period are thought to be required for entrainment though

535   there is not yet a consensus on how this is achieved. It is envisaged that changes in

536   circadian period are a result of phase adjustment of the oscillator. For example, a

537   phase advance will reduce the period of the cycle in which the advance occurred by

30

538 an amount equal to the phase advance (Johnson, 1992). Additionally, changes in the

539 velocity of the oscillator can affect period. Whilst changes in period are associated

540 with entrainment, it is not known if this is due to changes in velocity, phase or both

541 and whether these occur continuously or discontinuously (Daan, 2000). Our

542 discovery of a mutant that is specifically compromised in the ability to dynamically

543 alter circadian period and has altered entrained phase provides a tool to study the

544 mechanism of entrainment and the pathways of this essential feature of the circadian

545 oscillator. The study of how the circadian clock establishes a correct phase

546 relationship with the environment is essential to understand the role of the circadian

547 oscillator in the plant, because the timing of events within the diel cycle constitute the

548 likely evolutionary pressure that resulted in the emergence and optimisation of

549 circadian clocks.

550

551 **Materials and Methods**

552 **Plant materials and growth conditions**

553 *Arabidopsis thaliana* (Arabidopsis) ecotype Wassilewskija-2 (Ws-2) carrying

554 *CHLOROPHYLL A/B BINDING PROTEIN2:LUCIFERASE$^+$ (CAB2:LUC$^+$)* (Hall et al.,

555 2003) and transformed with *CaMV 35S:AEQUORIN (35S:AEQ)* was described

556 previously (Xu et al., 2007). *doc1-1* (Gil et al., 2001) was obtained from Nottingham

557 Arabidopsis Seed Stock Centre (Arabidopsis.org). *tir3-101* was a gift from Ottoline

558 Leyser (Sainsbury Laboratory at Cambridge University, Cambridge, UK). Plant

559 growth on agar or soil was as described previously (Xu et al., 2007).

560

561 **Mutagenesis**

31

562 Ws-2 seeds homozygous for *CAB2:LUC+* and *35S:AEQ* were mutagenized using

563 ethyl methane sulphonate (EMS; Sigma, UK). Seeds were suspended in 150 mM

564 EMS 0.1% (v/v) KCl for 4 hours in an atmosbag (Sigma, UK). Seeds were washed

565 three times in 100 mM sodium thiosulphate (Fisher, UK) before overnight

566 stratification at 4 $^{\circ}$C and sowing on soil at a density of 10 seeds per 4 cm^2 of soil.

567 Ten percent of the M1 seedlings had regions of chlorosis, indicative of EMS-induced

568 alterations to the genomic sequence. Seeds were harvested in 10 plant M2 pools.

569 100 seeds were screened from 160 pools, with a total of 16,000 M2 seeds screened.

570

571 **Circadian phenotyping**

572 *Luciferase imaging.* CAB2:LUC$^+$ luminescence was imaged from either clusters of 10

573 seedlings or individual seedlings (Haydon et al., 2017). Nicotinamide treatment was

574 applied by transferring membranes (1µm, Sefar) with seven-day-old seedlings to 10

575 mM nicotinamide-containing media. Clusters of plants were transferred to

576 nicotinamide-containing plates at seven days old using a sterile toothpick, lifting

577 plants under the hypocotyls. Treatment with luciferin and imaging with a Nightshade

578 CCD camera and imaging chamber (Berthold, UK) mounted with an 18 mm lens was

579 as described in Haydon et al (2017). Where the effect of light intensity was

580 investigated, the assay plates were covered with combinations of the following

581 neutral density filters: Lee Technical Filter #211 (Lee filters, UK) and Roscolux #397,

582 #97, #98 (Rosco, USA). Light intensity was measured using a Skye Quantum Sensor

583 (Skye instruments limited, Wales).

584

32

Delayed chlorophyll fluorescence imaging. Delayed chlorophyll fluorescence was measured from excised leaves of 28-day-old plants. Leaves were excised at the petiole and transplanted to fresh media in 25 well plates at dawn. The camera chamber was supplied with constant RB LED light at 70 µmol m^{-2} s^{-1} and was cooled to 20 ^{o}C. Measurements were automated and data extracted using IndiGO software (Berthold). Delayed chlorophyll fluorescence measurements were taken by acquiring luminescence for 60 seconds immediately following illumination.

Aequorin bioluminescence imaging. Aequorin bioluminescence was imaged from clusters of 15 seedlings as described in Hearn and Webb (2014).

Genetic Mapping

Segregation analysis. Crosses were made with paternal Ws-2 and maternal mutant. BC_1F_2 seedlings were screened as individual seedlings for circadian period of CAB2:LUC$^+$ on 10 mM nicotinamide. BC_2F_3 seedlings were screened as clusters of seedlings for circadian period of CAB2:LUC$^+$ in the presence or absence of 20 mM nicotinamide.

Mapping by sequencing. Genomic DNA was extracted from 20-day-old plants using the Qiagen Plant Maxi Kit and quantified using a nanodrop. Sequencing libraries were prepared using Ilumina Tru-seq. DNA was sequenced by VIB nucleomics (Ghent, Belgium) using an Illumina Hiseq 2000. Paired-end reads supplied in fastq format were trimmed using Fast X0.0.13 to remove reads with Q<20 or read length <35bp. Adapters were removed using cutadapt 1.2.1. Reads were further filtered to remove those with greater than 90% A content (poly-A reads), all ambiguous reads containing an N in any position, reads with <Q25, and artefact reads using FastX

33

609   0.0.13 and ShortRead 1.20.0. Contaminant reads were removed by discarding reads

610   that aligned to phix_illumina using Bowtie 2.1.0. Sequencing data in fastq format can

611   be obtained from NCBI SRA (ncbi.nlm.nih.gov/sra) under accession SRP119118.

612   Paired-end reads were aligned to the TAIR10 reference genome (Arabidopsis.org)

613   using Bowtie2 v.2.0.2 (Langmead 2010). SNP calling was performed using SAMtools

614   0.1.18 mpileup and bcftools (Li 2011). Vcf files were converted to SHORE format

615   using SHOREmap 2.1 convert. Allele frequency estimation and plots were generated

616   using SHOREmap backcross. The Ws-2 parental strain and Ws-2 1001 genomes

617   project

618   (http://1001genomes.org/data/MPI/MPIcollab2011/releases/current/strains/Ws-2/)

619   were used for background correction for BC_1F_2 in SHOREmap backcross. SNPs with

620   background frequency <16 were discarded. The workflow was automated in a

621   pipeline using bpipe 0.9.8.5. (Supplemental Table S3). Sliding allele frequencies

622   were generated for SNPs based on the R statistic in SHOREmap.

623   *SNP verification with dCAPS and Sanger sequencing.* Genomic DNA was extracted

624   from 300 µg plant material using the Plant Mini Kit (Qiagen). DNA was eluted into

625   150 µl of dH_2O (Sigma, UK). dCAPS was used to verify and genotype SNPs in wild-

626   type, BC_1F_2 pools and BC_2F_3 pedigrees. Primers and restriction enzymes used for

627   dCAPS were as follows, product sizes once amplicons had been digested are given

628   in   brackets: AT3G02260   F: TTAACATGTAATGTATTCCTCTGCA   R:

629   TCCAGTTTCCTCGTTACTGAC HindIII 300 bp (276 bp, 24 bp), AT3G02330 F:

630   GAGATTTCGTGACCTGGAACG R: GCATCTCTCGAATAAGCTCTAATG TasI   300

631   bp (276 bp, 24 bp), AT3G03070 F: CTAGTCGGCAATCACACCG R:

632   TTTCAGAAATGAACAATTCCCTGT BsmI 300 (275, 25). PCR reagents were

633   purchased as part of the Biotaq Kit (Bioline, UK) or as part of the Phusion

34

634 Polymerase Kit (NEB). PCR products were purified using the QIAquick PCR

635 Purification Kit (Qiagen) and quantified using a nanodrop 2000 (Thermo Scientific).

636 HindIII (Fisher Scientific), TasI (NEB) and BsmI (NEB) reactions were prepared for

637 100 µg DNA in their optimal buffers as specified in their instructions. Restriction

638 digestions were run in a Darwin thermocycler for 4 hours at 37 ^{o}C (HindIII) or 72 ^{o}C

639 (TasI, BsmI). Restriction enzyme reactions were deactivated by addition of 4 M TRIS

640 pH 8.4 purple loading dye (Bioline). Digested and undigested products were run on

641 2.5% and 4% fine molecular biology grade agarose (Bioline) 1x TAE buffer for

642 resolution of small fragments. Hyperladder 100 bp (Bioline) was used for size

643 comparison. Gels were imaged using a transilluminator controlled by GeneSnap

644 software with 80 s exposure. Alternatively, purified PCR products were Sanger

645 sequenced using reverse primers as the sequencing primers. Sequencing was

646 performed by Source Bioscience. Sequencing of SNPs was accepted if the

647 chromagraph had a quality score greater than 20.

648 **Isolation of RNA, determination of size and abundance**

649 *RNA extraction and reverse transcription.* RNA was extracted using RNeasy$^{®}$ Plant

650 Mini Kit (Qiagen) and RNase free DNase set (Qiagen). RNA was double eluted into

651 30 µl RNase-free H$_2$O. cDNA was generated from RNA using RevertAid First Strand

652 cDNA Synthesis Kit (K1622; Fermentas) using 0.5 µg RNA in a 10µl reaction

653 volume.

654 *RT-PCR and RT-qPCR.* Primers were generated using NCBI-primer BLAST as

655 follows: *AT3G02260*   F: GATGGTGAAGCTACTGAGCCT   R:

656 CTTCAGCTGGCTCCATAGCA (predicted product size for gDNA 458 bp and cDNA

657 316 bp), UBQ10   F: GGCCTTGTATAATCCCTGATGAATAAG   R:

35

658   AAAGAGATAACAGGAACGGAAACATAGT, CCA1   F:

659   GATGATGTTGAGGCGGATG R: TGGTGTTAACTGAGCTGTGAAG, TOC1   F:

660   TCTTCGCAGAATCCCTGTGAT R: GCTGCACCTAGCTTCAAGCA, PRR7   F:

661   GGAAACTTGGCGGATGAAAA R: CGAGGGCGTTGTTCTGCT, CHE   F:

662   TCCACCGGAAATGGTTTTTG R: GGCGGAAGCTTGCTGTTG. RT-PCR was

663   performed using the PCR settings and electrophoresis described above. RT-qPCR

664   was performed as previously described (Haydon et al., 2013).

665   Cytosolic-free calcium measurements

666   Plants grown on agar plates for 11 days were transferred to cuvettes and dosed with

667   coelenterazine to determine the free Ca^{2+} as described in Marti et al., (2013).

668   Nicotinamide guanine dinucleotide (NGD) assay of ADPR cyclase activity

669   ADPR cyclase activity was measured using the NGD assay as described in Abdul-

670   Awal et al., (2016) from 3- to 4-week-old plants grown on agar plates. Rosette tissue

671   (5-10 g) pooled from at least 25 rosettes was harvested as a single biological

672   replicate. Data were collected from three biological replicates.

673   Estimation of circadian parameters

674   Data were analysed using the BRASS plug-in for MS excel (http:// www.amillar.org) to

675   carry out Fast Fourier Transform Non-Linear Least Squares (FFT-NLLS) analysis and

676   manual phase estimation (Plautz et al., 1997). Rhythms were analysed for at least

677   three cycles in constant light after the first 24 hours. FFT-NLLS was performed with

678   period limits between 18 and 35 hours at 95% confidence level. Phase was calculated

679   using the BRASS peak time analysis function. Rhythms in RT-qPCR and microarray

680   time courses were analysed using JTK-cycle (Hughes et al., 2010) with period limits

681   between 20 and 32 hours.

36

Microarray analysis

Microarray datasets were downloaded from array express (E-GEOD-19271 and E-GEOD-50438) and the DIURNAL long day and short day expression sets.

Statistical tests

Two-sample T-tests, single-factor ANOVA and Chi-squared statistical tests were performed using MS Excel. Probability of rejecting the null hypothesis (p), calculated T-, F-, or Chi-squared statistic (T, F, x^2) and degrees of freedom (df) are quoted in the text for each analysis in the form (T=n df=n p=n).

Accession numbers

Sequence data for genes used in this study can be found in the Arabidopsis Genome Initiative or GenBank/EMBL databases under the following accession numbers: locus identifiers: BIG (AT3G02260), CAB2 (AT1G29920), CCA1 (AT2G46830), TOC1 (AT5G61380), CHE (AT5G08330), PRR7 (AT5G02810), ZTL (AT5G57360). Sequencing data in fastq format can be obtained from NCBI SRA (ncbi.nlm.nih.gov/sra) under accession SRP119118.

Supplemental Materials

Supplemental Figure S1. Dose response of circadian period to nicotinamide in Ws-2, *sin1* and son1.

Supplemental Figure S2. *son1* segregates with 3:433767 in BC$_2$F$_3$

37

703   **Supplemental Figure S3.** *son1* **plants do not have a circadian period phenotype**

704   **in the absence of nicotinamide**

705   **Supplemental Figure S4. Sequencing of cDNA for** *son1* **fragments**

706   **Supplemental Figure S5. The effect of nicotinamide on delayed chlorophyll**

707   **fluorescence rhythms in** *son1*, *doc1-1* **and** *tir3-101*

708   **Supplemental Figure S6. Allelism of** *son1* **and** *doc1* **is not due to ecotype**

709   **differences.**

710   **Supplemental Figure S7.** *doc1-1* **phenotype in** *son1*

711   **Supplemental Figure S8.** *BIG* **expression does not oscillate in long or short**

712   **day photoperiods or in constant light**

713   **Supplemental Figure S9. Circadian rhythms of CAB2:LUC$^+$ in** *BIG* **mutants**

714   **under different light intensities.**

715   **Supplemental Figure S10.** *son1* **does not adjust period due to photoperiod**

716   **entrainment**

717   **Supplemental Table S1 – Results of an M3 forward genetic screen for the effect**

718   **of nicotinamide on the circadian clock**

719   **Supplemental Table S2 -** *Arabidopsis thaliana* **circadian clock genes with**

720   **circadian and entrainment phenotypes.**

721   **Supplemental Table S3 – bpipe script for mapping by sequencing.**

722

723

38

725 We thank Ian Henderson for advice on genetic mapping. TH was supported by a

726 BBSRC CASE studentship 1090203 supported by Bayer Cropscience and BBSRC

727 Grant BB/M006212/1. MM was supported by a University of Cambridge Broodbank

728 Fellowship.

729

730

731

732

733 **Figure legends**

734 **Figure 1. A forward genetic screen separates period and amplitude effects of**

735 **nicotinamide. (A)** *CAB2:LUC*[+] rhythms in wild-type Ws-2 in the presence or

736 absence of 20 mM nicotinamide (NAM) in one entraining 12:12 light dark cycle (black

737 and white bars) and transferred into four days in constant light (white and grey bars)

738 at dawn (Zeitgeber [ZT] 0). Mean FFT-NLLS period estimates are shown ± SEM (n =

739 8). **(B)** Free-running circadian period and amplitude difference of M3 plants in a

740 forward genetic screen for the effect of 20 mM nicotinamide on circadian oscillations

741 of *CAB2:LUC*[+]. Period-insensitive mutants (*sin*) are indicated in green, period-

742 oversensitive mutants (*son*) in red and amplitude-sensitive mutants (*san*) in blue.

743 Plants with no detectable nicotinamide-response phenotype in the screen of the M3

744 population are shown in white, and mean wild-type Ws-2 ± SEM from all experiments

745 (n = 64) is shown overlaid in yellow. Data are pooled from eight separate

746 experiments. **(C)** *CAB2:LUC*[+] rhythms in *sin1*, *son1* and *san11* mutants (labelled in

747 **B**) in the presence or absence of 20 mM nicotinamide in one entraining 12:12 light

39

748 dark cycle and four days in 70 µmol m^{-2} s^{-1} constant light (n = 8). Data are

749 representative of two independent experiments in the M3 generation.

750

751

752 **Figure 2. A causal mutation in BIG underlies *son1***

753 **(A)** SHOREmap backcross mapping by sequencing analysis of *son1* generated from

754 25-fold coverage Illumina sequence data obtained from 25 BC$_1$F$_2$ individual plants

755 with the *son1* phenotype. Individual chromosomes are shown separately with allele

756 frequency sliding window generated with a moving average of 50 kb. A region with

757 allele frequency of one is found on the long arm of chromosome 3. **(B)** SNPs found

758 on chromosome 3 in *son1* with allele frequency of 1.0. Mutations highlighted in red

759 are predicted to cause a functional change in gene product. **(C)** BC$_2$F$_3$ segregation of

760 *son1* phenotype with mutation at 3:433767. Period difference in the presence of 20

761 mM nicotinamide was calculated by FFT-NLLS and plotted rounded to nearest 0.2 h.

762 Each line consisted of eight biological replicates, 45 lines were genotyped and

763 phenotyped. Mean and SD for each 3:433767 G-A genotypic sub-population (Wt,

764 heterozygous, and homozygous) were used to plot normal distributions overlaid onto

765 period histogram. **(D)** RT-PCR of *BIG* exons 11-12 showing the effect of *son1* on

766 *BIG* transcript isoforms. Lane 1 has Ws-2 genomic DNA product of predicted size

767 458bp. Lanes 2-4 have *son1* c-DNA products of 314 and 458 bp. Lanes 5-7 have

768 Ws-2 c-DNA product of 316bp. 1 Kb ladder annotated with fragment sizes is shown.

769 Independently isolated BC$_2$F$_3$ pedigrees were used. **(E)** Gene structure of

770 *At3G02260* (*BIG*), the potential UBR and ZZ type zinc finger domains and positions

771 of *son1* and *doc1-1* mutations are labelled. **(F)** Circadian period difference between

40

772   the presence and absence of 20 mM nicotinamide for delayed chlorophyll

773   fluorescence rhythms in Ws-2, *son1,* Col-0, *doc1-1* and *son1 doc1-1* F1. Period

774   estimates calculated using FFT-NLLS analysis (Mean ± SE shown, n = 10). Data are

775   representative of two independent experiments. **(G)** Delayed chlorophyll

776   fluorescence rhythm for *son1* x *doc1-1* F1 in the presence or absence of 20 mM

777   nicotinamide (NAM) across four days in constant light. White and grey bars show

778   subjective day and night. Mean ± SEM shown for n = 10. Data are representative of

779   two independent crosses. **(H)** Circadian period difference between the presence and

780   absence of 20 mM nicotinamide for delayed chlorophyll fluorescence rhythms of Col-

781   0, Ws-2, Col-0 x Ws-2 F1, *son1, doc1, son1* x ws-2 F1 and *doc1* x Ws-2 F1. Period

782   estimates calculated using FFT-NLLS analysis (Mean ± SEM shown, n = 10).

783

784   **Figure 3. *son1* affects circadian $[Ca^{2+}]_{cyt}$ signals**

785   Bioluminescence (photon counts/1500 seconds) from *son1* and Ws-2 expressing

786   *35S:AEQUORIN* across two light dark cycles and five days in constant 70 µmol m^{-2} s^{-}

787   ^{1} white light grown on 20 mM mannitol **(A)** or 20 mM nicotinamide (NAM) **(B)**. Mean

788   luminescence ± SEM shown, n = 8. Data are representative of three independent

789   experiments in the BC_2F_3 generation. **(C)** ADPR cyclase activity measured using

790   NGD assay at ZT4 in 70 µmol m^{-2} s^{-1} white light from 3-4 week old Ws-2 (white) and

791   *son1* (red) seedlings, mean of three biological replicates shown with SEM. **(D)**

792    $[Ca^{2+}]_{cyt}$ measured at zeitgeber (ZT) 4 and ZT 72 in constant 70 µmol m^{-2} s^{-1} white

793   light from 11 and 14 day old Ws-2 (white) and *son1* (red) seedlings respectively,

794   n=12. Data are representative of three independent experiments in the BC_2F_3

795   generation.

41

796

Figure 4. *son1* affects circadian clock gene expression in light dark cycles and constant light

(A) *CCA1, PRR7, TOC1* and *CHE* expression from *son1* (red) and Ws-2 (white) samples harvested immediately preceding dawn and dusk. ** represents significance at p<0.01 with T-test. Relative expression of genes normalised to UBQ10f expression is given ± standard deviation [n=3].**(B)** *CCA1*, *PRR7*, *TOC1* and *CHE* expression from Ws-2 and *son1* in the absence (left) and in the presence of 20 mM nicotinamide (right) across 48 hours in constant 70 µmol m^{-2} s^{-1} light from ZT24– ZT72. Relative expression of genes normalised to UBQ10f expression is given ± standard deviation [n=3]. Plants were grown as clusters of five plants for 11 days in light dark cycles prior to experiment.

808

Figure 5. *son1* affects dynamic circadian period adjustment by light and photoperiod

(A) Fluence response curve for circadian period of *CAB2:LUC$^+$* in Ws-2 and *son1* estimated in equal mixed red and blue light (Mean ± SEM, n = 8-12). Data are pooled from three independent experiments. **(B)** *CAB2:LUC$^+$* rhythm of *son1* and Ws-2 assayed over five days in constant 5 µmol m^{-2} s^{-1} equal mixed red and blue light (Mean ± SEM, n = 8). Data are representative of two independent experiments in the BC$_2$F$_3$ generation. In Figure 4a, the small error bars are obscured by symbols. **(C)** *CAB2:LUC$^+$* luminescence (counts s^{-1}) from *son1* (red) and Ws-2 (black) seedlings grown in 8:16, 12:12 and 16:8 photoperiods. Plants grown in 12:12 were treated with media supplemented with or without 20 mM nicotinamide (NAM) 2 days

42

820   prior to entrainment in camera chamber (mean ± SEM, n=8). Plants were grown in

821   entrainment conditions from germination and transferred to the camera chamber one

822   day before imaging, maintaining the same entrainment regime. Data are

823   representative of three independent experiments. **(D)** Peak time of *CAB2:LUC*[+] from

824   LD cycles in (C). Mean peak time of CAB2:LUC+ ± SEM plotted, n=8). ** indicates

825    $P<0.05$ with T-test.

826   **(E)** Photoperiod response curve for circadian period of *CAB2:LUC*[+] in Ws-2 and

827   *son1* estimated in equal mixed 80 µmol m^{-2} s^{-1} red and blue light (Mean ± SEM, n =

828   8). Data are pooled from two independent experiments. Plants were entrained in

829   either photoperiods of either 16, 12 or 8 hours prior to transfer to constant light. **(F)**

830   *CAB2:LUC*[+] rhythm of *son1* and Ws-2 entrained in 16:8 LD cycles and released into

831   constant light for five days (Mean ± SEM, n = 8).

832

833

43

Parsed Citations

Abdul-Awal, S.M., Hotta, C.T., Davey, M.P., Dodd, A.N., Smith A.G. and Webb, A.A.R. (2016) NO-mediated [Ca2+]cyt increases depend on ADP-ribosyl cyclase activity in Arabidopsis. Plant Physiology. 171, 623–631.
Pubmed: Author and Title
Google Scholar: Author Only Title Only Author and Title

Aschoff J. (1960) Exogenous and endogenous components in circadian rhythms. Cold Spring Harb Symp Quant Biol. 25, 11-28.
Pubmed: Author and Title
Google Scholar: Author Only Title Only Author and Title

Ashelford, K., Eriksson, M.E., Allen, C.M., D'Amore, R., Johansson, M., Gould, P., Kay, S., Millar, A.J., Hall, N., and Hall, A. (2011). Full genome re-sequencing reveals a novel circadian clock mutation in Arabidopsis. Genome Biol. 12, R28.
Pubmed: Author and Title
Google Scholar: Author Only Title Only Author and Title

Asher G, Gatfield D, Stratmann M, Reinke H, Dibner C, Kreppel F, Mostoslavsky R, Alt FW, and Schibler U. (2008) SIRT1 regulates circadian clock gene expression through PER2 deacetylation. Cell. 134, 317-28.
Pubmed: Author and Title
Google Scholar: Author Only Title Only Author and Title

Bachmair A, Finley D, Varshavsky A. (1986) In vivo half-life of a protein is a function of its amino-terminal residue. Science. 234, 179-186.
Pubmed: Author and Title
Google Scholar: Author Only Title Only Author and Title

Belzil, C., Asada, N., Ishiguro, K., Nakaya, T., Parsons, K., Pendolino, V., Neuermeyer, G., Mapelli, M., Nakatani, Y., Sanada, K., Nguyen, M.D. (2014) p600 regulates spindle orientation in apical neural progenitors and contributes to neurogenesis in the developing neocortex. Biol. Open. 3, 475-485.
Pubmed: Author and Title
Google Scholar: Author Only Title Only Author and Title

Belzil, C., Neumeyer, G., Vassilev, A.P., Yap, K.L., Konishi, H., Rivest, S., Sanada, K., Ikura, M., Nakatani, Y., Nguyen, M.D. (2013) A Ca2+-dependent mechanism of neuronal survival mediated by the microtubule-associated protein p600. J. Biol. Chem. 34, 24452-24464.
Pubmed: Author and Title
Google Scholar: Author Only Title Only Author and Title

Cha-Molstad, H., Yu, J.E., Feng, Z, Lee, S.H., Kim, J.G., Yang, P., Han, B., Sung, K.W., Yoo, Y.D., Hwang, J., et al. (2017) p62/SQSTM1/Sequesterome-1 is an N-recognin of the N-end rule pathway which modulates autophagosome biogenesis. Nat. Commun. 8, 102.
Pubmed: Author and Title
Google Scholar: Author Only Title Only Author and Title

Cui X, Lu F, Li Y, Xue Y, Kang Y, Zhang S, Qiu Q, Cui X, Zheng S, Liu B, Xu X, Cao X. (2013) Ubiquitin-specific proteases UBP12 and UBP13 act in circadian clock and photoperiodic flowering regulation in Arabidopsis. Plant Physiol. 162, 897-906.
Pubmed: Author and Title
Google Scholar: Author Only Title Only Author and Title

Daan S, (2000) Colin Pittendrigh, Jürgen Aschoff, and the natural entrainment of circadian systems. Biol. Rhythms. 15, 195–207.
Pubmed: Author and Title
Google Scholar: Author Only Title Only Author and Title

Dalchau N, Baek SJ, Briggs HM, Robertson FC, Dodd AN, Gardner MJ, Stancombe MA, Haydon MJ, Stan GB, Gonçalves JM, Webb AA. (2011) The circadian oscillator gene GIGANTEA mediates a long-term response of the Arabidopsis thaliana circadian clock to sucrose. Proc Natl Acad Sci U S A. 108, 5104-9.
Pubmed: Author and Title
Google Scholar: Author Only Title Only Author and Title

Dalchau N, Hubbard KE, Robertson FC, Hotta CT, Briggs HM, Stan GB, Gonçalves JM, and Webb AA. (2010) Correct biological timing in Arabidopsis requires multiple light-signaling pathways. Proc Natl Acad Sci U S A. 107, 13171-6.
Pubmed: Author and Title
Google Scholar: Author Only Title Only Author and Title

Dodd AN, Gardner MJ, Hotta CT, Hubbard KE, Dalchau N, Love J, Assie JM, Robertson FC, Jakobsen MK, Gonçalves J, Sanders D, and Webb AA. (2007) The Arabidopsis circadian clock incorporates a cADPR-based feedback loop. Science. 318, 1789-92.
Pubmed: Author and Title
Google Scholar: Author Only Title Only Author and Title

Endo M, Shimizu H, Nohales MA, Araki T, and Kay SA. (2014) Tissue-specific clocks in Arabidopsis show asymmetric coupling. Nature. 515:419-22.
Pubmed: Author and Title
Google Scholar: Author Only Title Only Author and Title

Farinas, B., and Mas, P. (2011). Functional implication of the MYB transcription factor RVE8/LCL5 in the circadian control of histone acetylation. Plant J. 66, 318–329.

Farré, E.M., Harmer, S.L., Harmon, F.G., Yanovsky, M.J., and Kay, S. a (2005). Overlapping and distinct roles of PRR7 and PRR9 in the Arabidopsis circadian clock. Curr. Biol. 15, 47–54.

Gibbs DJ, Bacardit J, Bachmair A, Holdsworth MJ. (2014) The eukaryotic N-end rule pathway: conserved mechanisms and diverse functions. Trends Cell Biol. 24, 603-611.

Gil P, Dewey E, Friml J, Zhao Y, Snowden KC, Putterill J, Palme K, Estelle M, Chory J. (2001) BIG: a calossin-like protein required for polar auxin transport in Arabidopsis. Genes Dev. 15, 1985-97.

Gould PD, Diaz P, Hogben C, Kusakina J, Salem R, Hartwell J, Hall A. (2009) Delayed fluorescence as a universal tool for the measurement of circadian rhythms in higher plants. Plant J. 58, 893-901.

Gray JA, Shalit-Kaneh A, Chu DN, Hsu PY, and Harmer SL. (2017) The REVEILLE Clock Genes Inhibit Growth of Juvenile and Adult Plants by Control of Cell Size. Plant Physiol. 173, 2308-2322.

Guo Y, and Tan J. (2013) Applications of delayed fluorescence from photosystem II. Sensors (Basel). 13, 17332-45.

Hall, A., Bastow, R.M., Davis, S.J., Hanano, S., McWatters, H.G., Hibberd, V., Doyle, M.R., Sung, S., Halliday, K.J., Amasino, R.M., et al. (2003). The TIME FOR COFFEE gene maintains the amplitude and timing of Arabidopsis circadian clocks. Plant Cell 15, 2719–2729.

Haydon MJ, Mielczarek O, Frank A, Román Á, and Webb AAR. (2017) Sucrose and Ethylene Signaling Interact to Modulate the Circadian Clock. Plant Physiol. 175, 947-958.

Haydon MJ, Mielczarek O, Robertson FC, Hubbard KE & Webb AAR. (2013) Photosynthetic entrainment of the Arabidopsis thaliana circadian clock. Nature. 502, 689–692.

Hazen, S.P., Schultz, T.F., Pruneda-Paz, J.L., Borevitz, J.O., Ecker, J.R., and Kay, S. A (2005). LUX ARRHYTHMO encodes a Myb domain protein essential for circadian rhythms. Proc. Natl. Acad. Sci. U. S. A. 102, 10387–10392.

He, J., Zhang, R.-X., Peng, K., Tagliavia, C., Li, S., Xue, S., Liu, A., Hu, H., Zhang, J., Hubbard, K. E., Held, K., McAinsh, M. R., Gray, J. E., Kudla, J., Schroeder, J. I., Liang, Y.-K. and Hetherington, A. M. (2018), The BIG protein distinguishes the process of CO2-induced stomatal closure from the inhibition of stomatal opening by CO2. New Phytol. doi:10.1111/nph.14957

Hearn TJ and Webb AA. (2014) Measuring circadian oscillations of cytosolic-free calcium in Arabidopsis thaliana. Methods Mol Biol. 1158, 215-26.

Hong, S., Song, H.-R., Lutz, K., Kerstetter, R. A, Michael, T.P., and McClung, C.R. (2010). Type II protein arginine methyltransferase 5 (PRMT5) is required for circadian period determination in Arabidopsis thaliana. Proc. Natl. Acad. Sci. U. S. A. 107, 21211–21216.

Huang WY, Wu YC, Pu HY, Wang Y, Jang GJ, and Wu SH. (2017) Plant dual-specificity tyrosine phosphorylation-regulated kinase optimizes light-regulated growth and development in Arabidopsis. Plant Cell Environ. 40, 1735-1747.

Hughes ME, Hogenesch JB, Kornacker K. (2010) JTK_CYCLE: an efficient nonparametric algorithm for detecting rhythmic components in genome-scale data sets. J Biol Rhythms. 25, 372-80.

Hunt L, Holdsworth MJ, and Gray JE. (2007) Nicotinamidase activity is important for germination. Plant J. 51, 341-51.

Johnson CH (1992) Phase response curves: What can they tell us about circadian clocks? In: Hiroshige T. and Honma K. (eds.), Circadian Clocks from Cell to Human Hokkaido Univ. Press, Sapporo. pp. 209-249,

Jones MA, Williams BA, McNicol J, Simpson CG, Brown JW, and Harmer SL. (2012) Mutation of Arabidopsis spliceosomal timekeeper locus1 causes circadian clock defects. Plant Cell. 24, 4066-82.

Kaczorowski, K. a, and Quail, P.H. (2003). Arabidopsis PSEUDO-RESPONSE REGULATOR7 is a signaling intermediate in phytochrome-regulated seedling deetiolation and phasing of the circadian clock. Plant Cell 15, 2654–2665.

Kanyuka K, Praekelt U, Franklin KA, Billingham OE, Hooley R, Whitelam GC, Halliday KJ. (2003) Mutations in the huge Arabidopsis gene BIG affect a range of hormone and light responses. Plant Journal. 35, 57-70.

Kaur, G., Subramanian, S. (2015) The UBR box and its relationship to binuclear RING-like treble clef zinc fingers. Biol. Direct. 10, 36

Kevei E, Gyula P, Hall A, Kozma-Bognár L, Kim WY, Eriksson ME, Tóth R, Hanano S, Fehér B, Southern MM, Bastow RM, Viczián A, Hibberd V, Davis SJ, Somers DE, Nagy F, and Millar AJ. (2006) Forward genetic analysis of the circadian clock separates the multiple functions of ZEITLUPE. Plant Physiol. 140, 933-45.

Kevei, É., Gyula, P., Fehér, B., Tóth, R., Viczián, A, Kircher, S., Rea, D., Dorjgotov, D., Schäfer, E., Millar, A.J., et al. (2007). Arabidopsis thaliana Circadian Clock Is Regulated by the Small GTPase LIP1. Curr. Biol. 17, 1456–1464.

Kim H, Kim Y, Yeom M, Lim J, Nam HG. (2016) Age-associated circadian period changes in Arabidopsis leaves. J Exp Bot. 67, 2665-73.

Kim J, Kim Y, Yeom M, Kim JH, Nam HG. (2008) FIONA1 is essential for regulating period length in the Arabidopsis circadian clock. Plant Cell. 20, 307-19.

Langmead, B. (2010). Aligning short sequencing reads with Bowtie. Curr. Protoc. Bioinformatics. 11, 11.7.

Li, H. (2011). A statistical framework for SNP calling, mutation discovery, association mapping and population genetical parameter estimation from sequencing data. Bioinformatics 27, 2987–2993.

Li, H.M., Altschmied, L., and Chory, J. (1994). Arabidopsis mutants define downstream branches in the phototransduction pathway. Genes Dev. 8, 339–349.

Love, J., Dodd, A.N., and Webb, A.A.R. (2004). Circadian and Diurnal Calcium Oscillations Encode Photoperiodic Information in Arabidopsis. Plant Cell 16, 956–966.

Malapeira, J., Khaitova, L.C., and Mas, P. (2012). Ordered changes in histone modifications at the core of the Arabidopsis circadian clock. Proc. Natl. Acad. Sci. U.S.A. 109, 21540-5.

Martí, M.C., Stancombe, M. A, and Webb, A. A R. (2013). Cell- and stimulus type-specific intracellular free Ca2+ signals in Arabidopsis. Plant Physiol. 163, 625–634.
Pubmed: Author and Title
Google Scholar: Author Only Title Only Author and Title

Martin-Tryon EL, Kreps JA, Harmer SL. (2007). GIGANTEA acts in blue light signaling and has biochemically separable roles in circadian clock and flowering time regulation. Plant Physiology. 143, 473-86.
Pubmed: Author and Title
Google Scholar: Author Only Title Only Author and Title

Martin-Tryon, E.L., and Harmer, S.L. (2008). XAP5 CIRCADIAN TIMEKEEPER coordinates light signals for proper timing of photomorphogenesis and the circadian clock in Arabidopsis. Plant Cell 20, 1244–1259.
Pubmed: Author and Title
Google Scholar: Author Only Title Only Author and Title

Masuda, W., Takenaka, S., Inageda, K., Nishina, H., Takahashi, K., Katada, T., Tsuyama, S., Inui, H., Miyatake, K., and Nakano, Y. (1997). Oscillation of ADPribosyl cyclase activity during the cell cycle and function of cyclic ADP-ribose in a unicellular organism, Euglena gracilis. FEBS Lett. 405, 104–106.
Pubmed: Author and Title
Google Scholar: Author Only Title Only Author and Title

Millar, a J., and Kay, S. a (1996). Integration of circadian and phototransduction pathways in the network controlling CAB gene transcription in Arabidopsis. Proc. Natl. Acad. Sci. U. S. A. 93, 15491–15496.
Pubmed: Author and Title
Google Scholar: Author Only Title Only Author and Title

Millar, A.J., Carré, I. A, Strayer, C. A, Chua, N.H., and Kay, S. A (1995). Circadian clock mutants in Arabidopsis identified by luciferase imaging. Science 267, 1161–1163.
Pubmed: Author and Title
Google Scholar: Author Only Title Only Author and Title

Millar, A. J., Carrington, J. T., Tee, W. V. and Hodge, S.K. (2015) Changing planetary rotation rescues the biological clock mutant lhy cca1 of Arabidopsis thaliana. bioRxiv, DOI: https://doi.org/10.1101/034629
Pubmed: Author and Title
Google Scholar: Author Only Title Only Author and Title

Mockler TC, Michael TP, Priest HD, Shen R, Sullivan CM, Givan SA, McEntee C, Kay S, and Chory J. (2007) THE DIURNAL PROJECT: Diurnal and circadian expression profiling, model-based pattern matching and promoter analysis. Cold Spring Harb Symp Quant Biol. 72, 353-63.
Pubmed: Author and Title
Google Scholar: Author Only Title Only Author and Title

Nakamichi N, Kita M, Ito S, Yamashino T, and Mizuno T. (2005) PSEUDO-RESPONSE REGULATORS, PRR9, PRR7 and PRR5, Together Play Essential Roles Close to the Circadian Clock of Arabidopsis thaliana. Plant and Cell Physiology 46, 686–698
Pubmed: Author and Title
Google Scholar: Author Only Title Only Author and Title

Nakatani, Y., Konishi, H., Vassilev, A, Kurooka, H., Ishiguro, K., Sawads, J., Ikura, T., Korsmeyer, S.J., Qin, J., Herlitz, A.M. (2005) p600 is a unique protein required for membrane morphogenesis and cell survival. Proc. Natl. Acad. Sci. U.S. A. 102, 15093-15098.
Pubmed: Author and Title
Google Scholar: Author Only Title Only Author and Title

Neill, J.S.O., Ooijen, G. Van, Dixon, L.E., Troein, C., Bouget, F., Reddy, A.B., and Millar, A.J. (2011). Circadian rhythms persist without transcription in a eukaryote. Nature. 469, 554–558.
Pubmed: Author and Title
Google Scholar: Author Only Title Only Author and Title

Panda, S., Poirier, G.G., and Kay, S. A (2002). tej defines a role for poly(ADP-ribosylation in establishing period length of the Arabidopsis circadian oscillator. Dev. Cell. 3, 51–61.
Pubmed: Author and Title
Google Scholar: Author Only Title Only Author and Title

Park, D.H. (1999). Control of Circadian Rhythms and Photoperiodic Flowering by the Arabidopsis GIGANTEA Gene. Science 285, 1579–1582.
Pubmed: Author and Title
Google Scholar: Author Only Title Only Author and Title

Plautz, J.D., Straume, M., Stanewsky, R., Jamison, C.F., Brandes, C., Dowse, H.B., Hall, J.C., and Kay, S.A. (1997). Quantitative Analysis of Drosophila period Gene Transcription in Living Animals. J. Biol. Rhythms 12, 204–217.
Pubmed: Author and Title
Google Scholar: Author Only Title Only Author and Title

Prusinkiewicz P, Crawford S, Smith RS, Ljung K, Bennett T, Ongaro V, Leyser O. (2009) Control of bud activation by an auxin transport switch. Proc Natl Acad Sci U S A. 106,17431-6.

Ramsey, K.M., Yoshino, J., Brace, C.S., Abrassart, D., Kobayashi, Y., Marcheva, B., Hong, H.-K., Chong, J.L., Buhr, E.D., Lee, C., et al. (2009). Circadian clock feedback cycle through NAMPT-mediated NAD+ biosynthesis. Science. 324, 651–654.

Richards, S., Hillman, T., Stern, M. (1996) Mutations in the Drosophila pushover gene confer increased neuronal excitability and spontaneous synaptic vesicle fusion. Genetics. 142, 1215-1223.

Ruegger M, Dewey E, Hobbie L, Brown D, Bernasconi P, Turner J, Muday G, Estelle M. (1997) Reduced naphthylphthalamic acid binding in the tir3 mutant of Arabidopsis is associated with a reduction in polar auxin transport and diverse morphological defects. Plant Cell. 9, 745-57.

Rugnone, M.L., Faigón Soverna, A, Sanchez, S.E., Schlaen, R.G., Hernando, C.E., Seymour, D.K., Mancini, E., Chernomoretz, A, Weigel, D., Más, P., et al. (2013). LNK genes integrate light and clock signaling networks at the core of the Arabidopsis oscillator. Proc. Natl. Acad. Sci. U. S. A. 110, 12120–12125.

Sahar, S., Nin, V., Barbosa, M.T., Chini, E.N., and Sassone-corsi, P. (2011). Altered behavioral and metabolic circadian rhythms in mice with disrupted NAD + oscillation. Aging. 3, 1–9.

Salomé PA, Weigel D, and McClung CR. (2010) The role of the Arabidopsis morning loop components CCA1, LHY, PRR7, and PRR9 in temperature compensation. Plant Cell. 22, 3650-61.

Schneeberger, K., Ossowski, S., Lanz, C., Juul, T., Petersen, A.H., Nielsen, K.L., Jørgensen, J.-E., Weigel, D., and Andersen, S.U. (2009). SHOREmap: simultaneous mapping and mutation identification by deep sequencing. Nat. Methods. 6, 550–551.

Sekelsy, J.J., McKim, K.S., Messina, L., French, R.L., Hurley, W.D., Arbel, T., Chin, G.M., Deneen, B., Force, S.J. et al. (1999) Identification of novel Drosophila meiotic genes recovered in a P-element screen. Genetics 152, 529-542

Seki M, Ohara T, Hearn TJ, Frank A, da Silva VCH, Caldana C, Webb AAR, Satake A. (2017) Adjustment of the Arabidopsis circadian oscillator by sugar signalling dictates the regulation of starch metabolism. Sci Rep. 16:8305.

Somers D.E., Devlin P.F., Kay S.A. (1998b) Phytochromes and cryptochromes in the entrainment of the Arabidopsis circadian clock. Science. 282, 1488-90.

Somers, D.E., Schultz, T.F., Milnamow, M., and Kay, S. A. (2000). ZEITLUPE encodes a novel clock-associated PAS protein from Arabidopsis. Cell 101, 319–329.

Somers, D.E., Webb, A.A, Pearson, M., and Kay, S. A. (1998a). The short-period mutant, toc1-1, alters circadian clock regulation of multiple outputs throughout development in Arabidopsis thaliana. Development 125, 485–494.

Takahashi N, Hirata Y, Aihara K, Mas P. (2015) A hierarchical multi-oscillator network orchestrates the Arabidopsis circadian system. Cell. 163,148-59.

Tasaki, T., Mulder, L.C.F., Iwamatsu, A, Lee, M.J., Davydov, I.V., Varshavsky, A, Muesing, M., Kwon, Y.T. (2005) A family of mammalian E3 ubiquitin ligases that contain the UBR box motif and recognise N-degrons. Mol. Cell Biol. 25, 7120-7136.

Tasaki, T., Zakrzewska, A, Dudgeon, D., Jiang, Y., Lazo, J.S., Kwon, Y.T. (2009) The substrate recognition domains of the N-end rule pathway. J. Biol. Chem. 284, 1884-1895.
Pubmed: Author and Title
Google Scholar: Author Only Title Only Author and Title

Wang X, Wu F, Xie Q, Wang H, Wang Y, Yue Y, Gahura O, Ma S, Liu L, Cao Y, Jiao Y, Puta F, McClung CR, Xu X, and Ma L. (2012) SKIP is a component of the spliceosome linking alternative splicing and the circadian clock in Arabidopsis. Plant Cell. 24, 3278-95.
Pubmed: Author and Title
Google Scholar: Author Only Title Only Author and Title

Wang Y, Wu JF, Nakamichi N, Sakakibara H, Nam HG, and Wu SH. (2011) LIGHT-REGULATED WD1 and PSEUDO-RESPONSE REGULATOR9 form a positive feedback regulatory loop in the Arabidopsis circadian clock. Plant Cell. 23, 486-98.
Pubmed: Author and Title
Google Scholar: Author Only Title Only Author and Title

Wu, J.-F., Wang, Y., and Wu, S.-H. (2008). Two new clock proteins, LWD1 and LWD2, regulate Arabidopsis photoperiodic flowering. Plant Physiol. 148, 948–959.
Pubmed: Author and Title
Google Scholar: Author Only Title Only Author and Title

Xie Q, Wang P, Liu X, Yuan L, Wang L, Zhang C, Li Y, Xing H, Zhi L, Yue Z, Zhao C, McClung CR, and Xu X. (2014) LNK1 and LNK2 are transcriptional coactivators in the Arabidopsis circadian oscillator. Plant Cell. 26, 2843-57.
Pubmed: Author and Title
Google Scholar: Author Only Title Only Author and Title

Xu, X., Hotta, C.T., Dodd, A.N., Love, J., Sharrock, R., Lee, Y.W., Xie, Q., Johnson, C.H., and Webb, A. A.R. (2007). Distinct light and clock modulation of cytosolic free Ca2+ oscillations and rhythmic CHLOROPHYLL A/B BINDING PROTEIN2 promoter activity in Arabidopsis. Plant Cell 19, 3474–3490.
Pubmed: Author and Title
Google Scholar: Author Only Title Only Author and Title

Xu, X-Z., Wes, P.D. Chen, H. Li, H-S., Yu, M., Morgan, S., Liu, Y., Montell, C. (1998) Retinal targets for calmodulin include proteins implicated in synaptic transmission. J. Biol. Chem. 273, 31297-31307.
Pubmed: Author and Title
Google Scholar: Author Only Title Only Author and Title

Yager, J., Richards, S., Hekmat-Scafe, D.S., Hurd, D.D., Sundaresan, V., Caprette, D.R., Saxton, W.M., Carlson, J.R., Stern, M. (2001) Control of Drosophila perineural glial growth by interacting neurotransmitter-mediated signalling pathways. Proc. Natl. Acad. Sci. U.S.A. 98, 10445-10450.
Pubmed: Author and Title
Google Scholar: Author Only Title Only Author and Title

Yap, K.L., Kim, J., Truong, K., Sherman, M., Yuan, T., Ikura, M. (2000) Calmodulin target database. J. Struct. Funct. Genom. 1, 8-14
Pubmed: Author and Title
Google Scholar: Author Only Title Only Author and Title

Yeang HY. (2015) Cycling of clock genes entrained to the solar rhythm enables plants to tell time: data from Arabidopsis. Ann Bot. 116, 15-22.
Pubmed: Author and Title
Google Scholar: Author Only Title Only Author and Title